Lund University GEM thesis series nr 20

Glacial lake flood hazard assessment and modelling: a GIS perspective

Maimoona Zehra Jawaid

2017
Department of Physical Geography and Ecosystem Science
Lund University
Sölvegatan 12
S-223 62 Lund
Sweden

LUND UNIVERSITY

UNIVERSITY OF TWENTE.
FACULTY OF GEO-INFORMATION SCIENCE AND EARTH OBSERVATION

Glacial lake flood hazard assessment and modelling: a GIS perspective

Maimoona Zehra Jawaid

Thesis submitted to the department of Physical Geography and Ecosystem Science, Lund University, in partial fulfilment of the requirements for the degree of Master of Science in Geo-information Science and Earth Observation for Environmental Modelling and Management

Thesis assessment board

Supervisor: Professor Petter Pilejsö (Lund University)

Exam committee:

Dr. Ali Mansourian (Lund University)

Associate Professor Emeritus, Jonas Åkerman (Lund University)

Disclaimer

This document describes work undertaken as part of a program of study at the University of Lund. All views and opinions expressed therein remain the sole responsibility of the author, and do not necessarily represent those of the institute.

Course title: Geo-information Science and Earth Observation for Environmental Modelling and Management (GEM)

Level: Master of Science (MSc)

Course duration: January 2017 until June 2017

Consortium partners:

The GEM master program is a cooperation of departments at 5 different universities:

University of Twente, ITC (The Netherlands)
University of Lund (Sweden)
University of Southampton (UK)
University of Warsaw (Poland)
University of Iceland (Iceland)

Abstract

High mountain regions have experienced decreased glacier stability due to varying climate conditions. As glaciers melt, they are being replaced by glacial lakes of different sizes, some of which are prone to outburst flooding, and have caused catastrophic damage to downstream settlements and infrastructure. The study proposes a framework for a first stage hazard assessment of glacial lakes using GIS techniques and a digital elevation model. It introduces a new dynamic flow runoff model in a glacial lake hazard context. Based on a triangular form based multiple flow algorithm, the model is used to estimate flood magnitude and hazard degree.

The assessment is applied to the Pho Chu sub-basin in the Himalayan region, Bhutan. The results show 6 lakes in the basin of area greater than 0.2 km^2 and 6 of them classified as potentially hazardous by at least one hazard indicator. It is found that there could be different ways to determine moraine dam steepness and several spatial methods are attempted. The possibility of measuring moraine dimensions is limited by the digital elevation model's resolution. The assessment method can be further improved by including a hazard indicator for rock avalanches. Flood routing from Raphstreng lake is modelled over a pilot area in the sub-basin to demonstrate the application, assuming partial lake drainage. The maximum flood depth reached during model run time of 300 minutes, mostly falls between 1 to 15 m. Spatially concentrated in the main river channel, the flood extent enters the first settlement area at about 140 minutes from the start time. Rating hazard degree, the results show that most of the inundated extent fell under the extremely hazardous category. Where flood data are available from post-flood field surveys, it is recommended that the model be validated. A useful aspect of implementing the dynamic model in the future is that analysis of flood arrival time with respect to different settlements and infrastructure can be carried out, as water depths in the study area are saved for each time step.

Acknowledgements

I want to thank Petter Pilesjö, my supervisor, for his encouragement, ideas, good advice and making me think. I would also like to thank Hampus Nilsson for agreeing to use the dynamic model in this study, for answering all questions about the model and giving useful suggestions. I appreciate Per Moller for taking the time out for our discussion about moraines and glaciers.

It wouldn’t have been possible to reach the end of my thesis and programme without my family’s support and well wishes. Such an exciting part of the last two years, Melissa, Renata, Geert, Fabricio, Kaaviya, Pepicek, Misa, Xime, Moni, Nina, Jirka, Arne, Xu, Emma, John and more wonderful friends I got to know during the Erasmus programme - they are truly unforgettable! Cynthia and Michael, for their incredible warm welcome and support, Shabana, for making me finish my application, Alizay and Meherunissa, who supported me when I needed this the most, my friends from home, my parents for being the best people I know!

For inspiration to pursue career and academic goals, I am grateful to Ali Dehlavi, Aysha Jamall, Rab Nawaz, Adnan Khan.

Finally, a thank you to the amazing faculty and GEM team at ITC and Lund University!

1 Table of Contents

1 Introduction

High mountain regions have experienced decreased glacier stability due to varying climate conditions (Casassa et al. 2014). As glaciers melt, they are being replaced by glacial lakes of different sizes, some of which are prone to outburst flooding, and have caused catastrophic damage to downstream settlements and infrastructure (Rounce et al. 2016). Carrying water and sediment, floods from moraine dammed lakes can travel more than hundred kilometers at high velocities (Worni et al. 2014). Moraine dams, formed during the Little Ice Age (conventionally 16th–mid 19th century period of glacial advance), are glacial landforms composed of loose sediments, granular materials left behind by advancing glacial ice (Section 2.1). Released floodwaters are mixed with rock, mud, glacial sediments and can erode the banks along the flood path (Iturrizaga 2011).

Previous events of lake flooding have been recorded in high mountain regions of the world including the Peruvian Andes, Himalayas, Hindu Kush and Karakoram mountain ranges. In 1941, the Laguna Palcacocha lake outburst resulted in 6000 people losing their lives in the city of Huaraz, Peru (Huggel et al. 2002). Peru has experienced more than 21 glacial lake floods in the last 65 years (Wang et al. 2015). This includes the Lake Safuna Alta flood in 2002 set off by a rock avalanche (Hubbard et al. 2005) and the 2010 glacial lake outburst flood in Chucchún valley, Cordillera Blanca, when a glacial block crashed into the lake (Vilímek et al. 2015).

In the Himalayan region, some of the most damaging events have occurred (Worni et al. 2013). Table 1 shows some instances of glacial lake flood outbursts in the region, usually referred to as *GLOFs*. Peak flows for moraine dammed lakes have reached up to 2350 m^3/sec. The outburst of the Luggye Tsho in 1994 was a disastrous event in terms of life and land in Bhutan. This flood affected areas downstream reaching a height of 4 m measured 85 km from lake, and released an estimated total volume of 48 million m^3 of water (Richardson & Reynolds 2000). 21 people lost lives, 91 households were affected and 965 acres of pasture land were washed away in the Punakha - Wangdue valley (ICIMOD 2011). The International Centre for Integrated Mountain Development (ICIMOD) reports 25 lakes in Bhutan which have been identified as potentially dangerous (GLOF International Conference Report, 2012). The Pho Chu sub-basin in Bhutan alone has recorded 4 events since 1950, although documented details of only the 1994 event are known (Osti et al. 2013).

Moreover, 14 events have been recorded in Nepal and 10 events in Tibet, China (ICIMOD 2011). In Nepal, an extensively documented event concerns the Dig Tsho lake, which took place in 1985. The lake held about 5 million m^3 of water with another 1–2 million m^3 of dead ice. Water flowed over the moraine dam when an ice avalanche hit the lake. Within a few hours, lake water completely drained downstream with a peak

discharge of about 2000 m^3/s (Kattelmann 2003). The author notes that nearly all GLOF events have taken place around months of July, August or September.

Table 1. Examples of past glacial flood events recorded in the Himalayan region. Adapted from X. Wang et al. (2012) and *Wang et al. (2015).

Lake name, Country	Flood date	Volume (10^6 m^3)	Peak discharge (m^3/sec)
Longdaco, China	1964.8.25	10.8	-
Zhangzangbu, China	1981.7.11	19	1600
Gelhaipco, China	1964.9.21	23.4	4500
Qunbixiamaco, China	1940.7.10	12.4	3690
Damenlahecho, China	1964.9.26	2	2000
Degapuco, China	2002.9.18	-	-
Chubung, Nepal	1991.7.12	-	-
Cirenmaco, China*	1981	-	-
Dig Tsho, Nepal	1985.8.4	5	1600 - 2350

1.1 Aim

The aim of this study is to develop a first stage general hazard and vulnerability assessment framework for glacial lake flood hazard. Research will address the following sub-objectives:

Implement criterion to assess the hazard potential of a glacial lake
Building upon previous studies of identifying potential dangerous lakes, a decision criterion is implemented which can be applied to moraine dammed glacial lakes using a digital elevation model (DEM), spatial techniques and visual interpretation. Selected hazard indicators are lake area, moraine steepness, distance to glacier and glacier end slope. The indicators are selected based on having been used for preliminary hazard assessment in previous studies and those that are possible to extract from available data. Bhutan's river sub-basin Pho Chu is chosen as the pilot site for the indicators to be applied to lakes.

Estimate glacial lake flood with a dynamic runoff model
Hazard events are commonly assessed based on the size of impact and probability of occurrence (Schmidt, 2011). The impact variables in this case will be flood water maximum depth, velocity and extent. A distributed hydrological flow model based on a multiple flow direction algorithm will be applied to estimate the extent of possible flooding and water depth (Nilsson 2017; Pilesjö & Hasan 2014). A potentially hazardous lake site in the Pho Chu sub basin, Bhutan, is used for flood modelling.

Vulnerability Mapping

Flood model results will determine the degree of hazard impact at downstream settlement areas that are likely to be affected by the flood. Spatial distribution of flood depth and velocity will be used to map semi-qualitative levels of the degree of hazard.

2 Background

2.1 Moraines and glacial lakes

Moraines are landforms in glacial environments, consisting of loose sediments or *till*, deposited or deformed by glacier movement. They are mainly composed of an unsorted "mixture of clay, silt, sand, pebbles, cobbles and boulders" (Canadian Encyclopedia). There are different moraine types, classified by their position with respect to the glacier or the processes by which they are formed (Schomacker 2011). Usually they are tens of meters high, and have low width-to-height ratios of about 0.1 to 0.2. They may exist as one, two or more moraine structures, formed during consequent glacial advances (Clague & Evans 2000). Terminal moraines, an example illustrated in Figure 1, are prominent outermost edges which mark the maximum extent of glacier reach. Recessional moraines are younger and nested within and parallel to terminal moraines (Benn and Evans 2010). Lateral moraines form on the sides of a glacier.

Figure 1. Terminal moraine at the foot of a small glacier on the north slope of Jackson Mountain, Glacier National Park, Montana. Source: Stebinger, E.C., U.S. Geological Survey.

Often located in remote areas, difficult to access, "a glacial lake is defined as water mass existing in a sufficient amount and extending with a free surface in, under, beside, and/or in front of a glacier and originating from glacier activities and/or retreating processes of a glacier" (Jain et al. 2015). Glacial lakes are named by their position with respect to the glacier or how they are enclosed. *Supraglacial lakes* are those that form on a glacier's surface. *Subglacial lakes* are found under a glacier. *Englacial water bodies* are small volumes of meltwater trapped in channels inside the glacier. *Ice dammed glacial lakes* form when glacial drainage is halted by an advancing or retreating glacier (Benn and Evans 2010).

In this study, we focus on *proglacial lakes* which are bordered by moraines, hereon after referred to as *moraine dammed lakes*. According to authors Tweed and Carrivick (2015), a proglacial lake is another term for a water body which has formed at the end of a glacier from meltwater and can be bordered by moraines, ice or bedrock. Their presence affects the meltwater flow from glaciers and results in sedimentation accumulating within the lakes. Their evolution is related to glacier advance and retreat, in turn influenced by the changing climate. They can expand quickly. Usually, they form near glaciers covered with rock fragments and sediments because covered glacier ends tend to deteriorate and create depressions. The de-glaciated basin is then filled

with meltwater. Lake volume may increase with time until reaching a constant as water naturally drains through or over the moraine or until it is drained from an external trigger event (Westoby et al. 2014a).

Komori (2008) sums up the expansion process of glacial lakes formed from small valley glaciers. From when they are formed, they may go through three stages. First, they appear as small supraglacial ponds. Lakes in the second stage transition to form a single merged lake. The first two stages together last typically 10 to 20 years. Stage three is characterized by stable expansion upstream, while the lower edge of the lake remains in the same location, obstructed by a natural barrier. For instance, Tsho Rolpa lake has grown to be the largest moraine dammed lake in Nepal, from a few small ponds observed in 1957 to a single lake 3.5 km long and 0.5 wide, and maximum depth of 135 m in 1999 (Benn and Evans 2010). These three stages, however, do not apply to lakes forming in large valley glaciers.

In the region spanning Pamirs, Hindu Kush, Karakoram, Himalayas and the Tibetan Plateau, Zhang et al. (2015) found an increasing number of glacial lakes following an analysis of Landsat imagery from different years. From years 2009-2011, 5701 glacial lakes were delineated. In the same study, lakes which were fed by glaciers showed greater area changes than those that were not. Area change trends were shown to be coincident with increasing temperatures and decreasing mass balance of glaciers.

2.2 Flood causes and characteristics

Glacial lake floods from moraine dammed lakes are consequences of a chain of events leading to moraine dam failure or dam overflow. Figure 2 illustrates the potential triggers, conditioning factors and different stages of a lake outburst. Formed on slopes descending below glaciers and rock faces, the lake rests on loose sediments. Lake outbursts may be set off by external triggers causing displacement waves which erode the moraine. Triggers could be rock or ice avalanches, glacier calving into the lake, seismic activity or atmospheric activity (Westoby et al. 2014a). Glacier calving refers to the process when chunks of ice break off from the end of a glacier (Alaska Satellite Facility 2017). The most common trigger leading to dam breaching is due to glacier calving or avalanches setting off impact waves (Jain et al. 2015).

Conditioning factors which contribute to moraine weakness could be piping or ground water flow, the moraine dam geometry such as low width-to-height ratio and low freeboard, permafrost or buried ice core presence in the moraine (Westoby et al. 2014a). Piping refers to subsurface erosion of soils which creates a channel for flow to escape (Masannat, 1980). Moraine structures with buried ice can quickly be destabilized if the ice melts. The width of the dam is measured horizontally from the lake shore to the moraine's farthest extent. A low width-to-height dam ratio implies a narrow, less stable structure compared to a wider dam of lower elevation. Freeboard refers to the height between the lake surface and the top of the dam. A low freeboard makes a lake more

susceptible to waves caused by external triggers. Heavy rainfall or snowmelt or rapid influx of drainage from the glacier can raise the water level of the lake and lead to an outburst (Clague & Evans 2000).

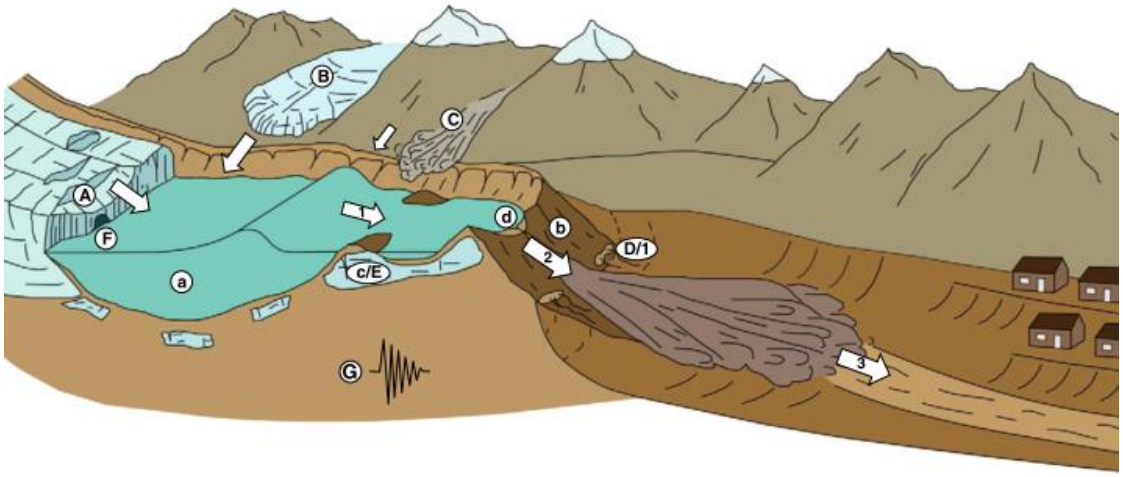

Figure 2. Schematic of a hazardous moraine-dammed glacial lake. **Potential triggers**: (A) glacier calving; (B) icefall from hanging glaciers; (C) rock, ice or snow avalanches; (D) dam piping; (E) ice cored-moraine degradation; (F) rapid input of water from supra-, en- or sub-glacial sources; (G) Seismicity. **Conditioning factors** for dam failure: (a) large lake volume; (b) low-width-to-height dam ratio; (c) degradation of buried ice in the moraine; (d) limited dam freeboard; **Key stages of a lake outburst:** (1) propagation of displacement waves and/or piping through the dam; (2) breach formation; (3) propagation of flood downstream. Adapted from Westoby et al. (2014a) and Richardson and Reynolds (2000). Figure reprinted from *Earth Science Reviews*, 134 (2014), Westoby et al. (2014), Modelling outburst floods from moraine-dammed glacial lakes, p. 139, Copyright (2014), with permission from Elsevier.

The moraine spillway is the one of the main factors in determining the threat of a lake. Signs of moraine likelihood to failure can be inferred from moraine steepness, absence of a lake outflow channel and evidence of seepage. Also, steep glacier slopes near the lake increase the likelihood of ice avalanches (Clague & Evans 2000).

At the moraine breach, the nature of flood can be catastrophic, and results in a debris fan to form below it (Richardson & Reynolds 2000). Kattelmann (2003) notes that in a short amount of time, worst case events have let millions of cubic meters of water to escape downstream. Significant amounts of moraine sediments are collected in the first few hundred meters and flatter areas. The flow can mobilize sediments and valley slope particles as well as vegetation. This can also set off landslides as lower valley slopes are disturbed.

Compared to snowmelt or rainfall runoff, glacial lake floods can be much larger in magnitude in the same catchment areas (Post and Mayo 1971). Usually, they peak suddenly and then decline gradually downstream (Clague & Evans 2000). Currently,

actual measured hydrographs of such floods are recorded at a distance of tens or hundreds of kilometers away from the source, due to the remoteness and the damaging nature of the events (Westoby et al. 2014). They decrease with distance downstream because the flood wave goes through frictional diffusion, while rainfall triggered events usually increase downstream as the drainage area increases (Cenderelli & Wohl 2001).

Other kinds of glacial floods may occur from ice dammed lakes but they have different initiation processes from moraine dammed lakes (Richardson & Reynolds 2000). Drainage from ice dammed lakes may not destroy the dam, as the water may escape through subglacial channels (Benn and Evans 2010).

2.3 Hazard assessment

A number of studies have applied techniques based on remote sensing and geographic information systems (GIS) for a first order hazard assessment, which are especially useful in difficult to access and data scarce regions (Quincey et al. 2007; Huggel et al. 2004; Rounce et al. 2016; Wang et al. 2011). Because of the low feasibility of studying each lake in the field, a first stage assessment is often carried out through remote sources and selected indicators to narrow down potentially hazardous lake sites. A more detailed assessment after this is assumed and requires site specific knowledge. So far, multiple approaches to such an assessment have been proposed, though the indicators significant for consideration are repeatedly used in different studies. Table 2 lists a summary of the most frequently used indicators (Rounce et al. 2016). The indicators used may be dependent on the availability and resolution of data.

Table 2. Most frequently used indicators in past assessments for glacial lake hazard potential. Source: Adapted from Rounce et al. (2016); Emmer and Vilimek (2013).

Hazard indicators	**Number of studies**
Moraine stability	
Moraine width-to-height ratio	9
Buried ice in the moraine	8
Piping/seepage through the moraine	7
Moraine dam freeboard	6
Moraine dam type or composition	5
Steepness of moraine	5
Potential trigger events	
Mass movement into lake	11
Distance between lake and glacier	8
Glacier snout steepness	6
Seismic activity	3
Extreme temperature/precipitation	3

Downstream impact	
Lake area and/or volume	6
Flood inundation model	5

Richardson & Reynolds (2000) state that the combined effect of "lake volume, dam width, freeboard height and buried ice-cores, with evidence of human vulnerability" can be used to infer the hazard potential of a lake. Lake volume is the main variable to estimate peak flood discharge from empirical relationships. Other authors assign qualitative probability to lake outburst occurrence based on dam type and dam geometry. The probability of avalanche events and proximity of water supply to glacier bed are also considered (Huggel et al. 2004).

Alternative to measuring the width-to-height ratio of the dam, Fujita et al. (2013) came up with a single parameter of potential flood volume, calculated from the depression angle between the flat lake surface and the surrounding terrain. They proposed a threshold angle of 10 degrees for the steepness of the lake front area, representing moraine steepness. This was based on an analysis of historical satellite images of 5 lakes in Bhutan, Nepal, Tibet, before dam failure had occurred.

McKillop & Clague (2007) performed logistic regression modelling using eighteen candidate variables to arrive at significant hazard predictor variables. They included data from 20 drained lakes and 166 undrained lakes greater than 1 ha in the Coast mountains of British Columbia. Four significant variables were found – moraine height-to-width ratio (highly significant), presence of ice core in moraine, lake area, and moraine rock type. Validating the model yielded 99% and 40% prediction accuracy for undrained and drained lakes respectively when the probability threshold was 50%. A better accuracy was achieved when the probability threshold was lowered.

2.4 Flood modelling

The glacial lake flood phenomenon is frequently described as a complex chain reaction. In terms of modelling, Westoby and colleagues (2014a) note that processes are broken down into the following components:

1. Triggers such as mass movement into the lake;
2. Moraine dam breaching;
3. Flood propagation,

Few studies have attempted to model the whole process chain of the lake flood event. It is more common that processes are modelled separately, with the output from one being used as an initial condition in the next.

2.4.1 Dam breach models

Dam breach models may be empirical or deterministic. They calculate flood peak discharge at the dam break location and time to peak. Empirical models have been often used, though they do not consider basic hydraulic principles associated with breach expansion, but rely on regression from historical cases (Westoby et al. 2014a). Deterministic models use numerical sediment-transport relationships to represent erosion processes which cause the dam to break and the dam breach width expansion (Rivas et al. 2015). Inputs to numerical models such as HR-BREACH may require detailed dam geometry characteristics (Westoby et al. 2014b).

2.4.2 Flood inundation models

Predicting frequencies of floods from storms is usually done with the help of past streamflow records. For glacial lake floods, different methods are applied as the discharges are much higher and originate from a single source, capable of changing the characteristics of the drainage basin itself (Post & Mayo, 1971).

Physically based numerical models for flood inundation, after the moraine breach, mostly include one-dimensional (1-D) or two-dimensional (2-D) models, which assume different versions of the Navier Stokes equation for fluid flow. HEC-RAS, Mike 11, NWS-FLDWAV, BOSS DAMBRK, FLO-2D, RAMMS, SOBEK are model examples (Westoby et al. 2014a).

For instance, RAMMS simulation software uses a second order numerical solution of shallow water equations and the specification of a hydrograph to model debris flow (Frey et al. 2016). The HEC-RAS model uses energy and momentum flow equations for unsteady or steady flow through a channel.

2.4.2.1 GIS based flow routing models

Two flood routing algorithms over a grid based DEM have been used by Huggel et al. (2003) to model glacial debris flow in the Alps, with slight modifications. The frequently used single flow direction algorithm allows a grid cell to transfer flow to a side neighbor or to a diagonal neighboring cell, whichever has the steepest slope. The single flow algorithm is termed the *D8 method* by O'Callaghan & Mark (1984). To overcome the simplicity of the single flow method, the multiple flow model, developed by Quin et al. (1991), distributes flow to several lower neighbors by assigning weights in proportion to the slope. The authors found that the multiple flow model was more robust for a regional scale hazard assessment, even though the results are limited to DEM quality and accuracy.

2.5 Vulnerability

Papathoma-Köhle et al. (2011) define vulnerability as ‘‘the degree of loss of a specific element at risk to a hazard of a given magnitude.” Usually, vulnerability is ranked with values between 0 and 1, following a quantitative approach. As reviewed by the authors, vulnerability to flood events is most commonly linked to inundations depths. Flow velocity is an additional parameter considered for dynamic floods in alpine environments. In integrated assessments, vulnerability is frequently associated with hazard and risk.

It is now possible to use thematic maps to combine different factors to spatially delineate vulnerability. Indicators of social, economic and ecological categories, weighted in varying importance, are combined to present a spatial representation of vulnerability (Mejía-Navarro et al. 1994). Assigning weights and vulnerability scores are done after consultation with experts for a specific area.

Some authors use measures of hazard, physical exposure and adaptive capacity of communities or ability to recover from hazard when classifying vulnerability (Shrestha 2005), while others have noted that measuring vulnerability also involves taking into account buildings and their value (Papathoma-Köhle et al. 2011).

3 Methodology

The hazard assessment framework is applied to the Pho Chu sub basin in the Himalayan region, Bhutan. A remote location at very high elevation, the area hosts many glacial lakes and is suitable for a study of moraine dammed lakes. Generally retreating, glaciers in this region are known to be several types - cirque, niche, outlet and valley glaciers. Supraglacial ponds are well known to appear temporarily on Himalayan glaciers (Richardson & Reynolds 2000). The study area is described further in section 3.3.2.

3.1 Data

Data that were freely available was chosen for this study. Table 3 summarizes the type of data used and its sources.

The Advanced Spaceborne Thermal Emission and Reflection Radiometer (ASTER) sensor, operated by NASA, has captured images with global coverage. Stereo pairs of these images have been used to construct a global digital elevation model (GDEM) with a resolution of 30 by 30 m. Grid based elevation data are freely available in Georeferenced Tagged Image File Format (GeoTIFF). The second version of the GDEM, released in October 2011, is a product of METI and NASA. The images used for this research are referenced with the WGS84 1984 World Geodetic System.

"Glacier and Lake Inventory in Bhutan" was downloaded from the Japan Aerospace Exploration Agency (JAXA) website (Ukita et al, 2011; Tandono et al, 2012; Nagai et al, 2016). The dataset was processed and developed under Japan Science and Technology Agency (JST) and Japan International Cooperation Agency (JICA). In addition to glacier extents in the Bhutan Himalayan region, lakes greater than 0.01 km^2, which were supraglacial or within 2 km of a moraine were included in the inventory (Anon 2016).

Settlements points for Bhutan were downloaded from the Humanitarian Data Exchange website (2015), contributed by the UN Office for Humanitarian affairs, whereas the original source is Open Street Map (OSM). When Google Earth imagery had cloud cover, World imagery basemap from ArcGIS was used. World Imagery captures satellite and aerial imagery from multiple sources. TerraColor and SPOT images are included.

Table 3. Summary of data used for hazard assessment and flood modelling.

	Satellite	Sensor	Resolution/ Format	Date	Source, version	Main attributes
DEM	Terra	ASTER	30 m, .tiff	Released October 2011	USGS Earth Explorer, GDEM v2	Elevation
Glacier and lake inventory, Bhutan	Advanced Land Observing Satellite (ALOS)	PRISM and AVNIR-2	2.5 and 10 m, Polygon shapefile	ALOS operated from 2006-2011	JAXA, Version 16.11 - Updated November 2016	Lake elevation, Area, Name and ID, River sub-basin
Settlements, Bhutan			Point shapefile	June 5, 2015	Global Discovery, Open Street Map	Village name, Administrative level 1 name, Administrative level 2 name
Google Earth imagery	Landsat			2011-2012		
World Imagery	multiple		15m (terracolor) 2.5m (SPOT)		Esri, DigitalGlobe, GeoEye, Earthstar Geographics, CNES/Airbus DS, USDA, USGS, AeroGRID, IGN, and the GIS User Community	

3.2 Hazard assessment

Based on literature review and the most frequently used parameters, geomorphological hazard indicators are selected for a first stage assessment with the following criteria:

- Indicators can be derived from a DEM or satellite imagery;
- They account for the stability of the moraine, which is a crucial factor for indicating hazard potential;
- They account for the likelihood of external trigger events, such as ice avalanches or glacier calving or sudden release of glacial meltwater.

Additionally, lake type is determined to exclude lakes which are not moraine dammed. Trigger events such as earthquakes and extreme temperature or rainfall could not be considered. Table 4 lists selected indicators for determining hazard potential and limits used to define hazard classes. We consider a moraine dammed lake to be potentially hazardous if its characteristics fall in any one of the moderate or high classes.

Table 4. Hazard potential indicators for glacial lake moraine stability and external triggers for glacial lake outburst. A moraine dammed lake is classified as potentially hazardous if its characteristics fall in any one of the moderate or high classes.

Hazard potential indicator	Thresholds	Hazard potential	Source
Lake Area	>0.2 km^2	High	(Che et al. 2004).
	<0.2 km^2	Low	
Moraine steepness	>15	High	(Fujita et al. 2013; Iribarren et al. 2014)
	8-15	Moderate	
	<8 degrees	Low	
Distance between lake boundary and glacier	>500m	Low	(Wang et al. 2011)
	<500m	High	
	In contact	Very high	
Glacier end steepness	>25 degrees	High	(Bolch et al. 2011)
	<25 degrees	Low	

The glacier and lake inventory dataset groups lakes by sub-basins in Bhutan. Pho Chu sub basin lakes are selected to determine the following:

Lake type: Google Earth imagery and ArcGIS terrain base map are used for visual interpretation to determine whether the lakes are moraine dammed (Figure 3). Visual interpretation of moraine, area and glaciers around the lake is carried out. Moraine dammed lakes are identified through their position relative to glaciers and visible presence of moraines around their boundaries.

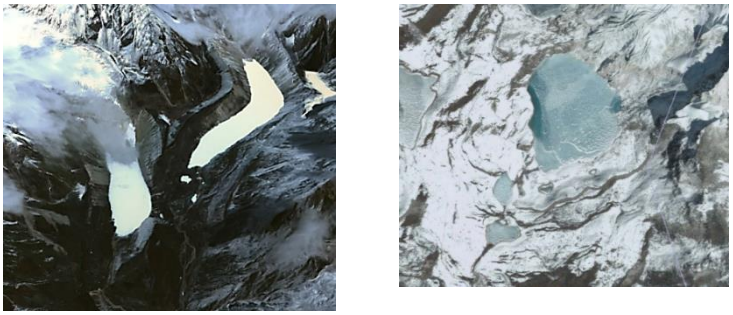

Figure 3. Google Earth image examples of moraine dammed lakes (left) and supraglacial lake (right) in the Pho Chu sub basin, Bhutan. If a lake is observed at the end of a glacier with a visible moraine surrounding it, it is classified as moraine dammed.

Lake Area: Greater lake area implies greater volume of water available for flood. Lakes of area greater than 0.2 km^2 have been considered as potentially dangerous (Che et al. 2004). Other authors have used limits of 0.1 - 0.25 km^2 (Aggarwal et al. 2013; Bolch et al. 2011; Khanal et al. 2015). We choose a limit of 0.2 km^2 and all lakes of area greater than this limit are subset from the lake inventory for further analysis.

Moraine steepness: As an alternate measurement of the moraine dam width-to-height ratio, the angle of depression from the lake has been used (Fujita et al. 2013). The angle of depression is an indicator of the steepness of the moraine and they use a threshold of 10 degrees to classify hazard potential. Another study uses classes of less than 8, 8-15, greater than 15 degrees to define low, moderate, high hazard respectively, based on analyzing 16 historic outburst cases in Pantagonia, Chile (Iribarren et al. 2014). We use the latter set of classes as we use a slightly different method from Fujita et al. (2013) to determine moraine steepness.

An estimate of the moraine (front) steepness is obtained by defining a lake front area for the identified moraine dammed lakes. Since defining a lake front area as done by Fujita et al. (2013) requires more parameters to be measured such as the mean depth of the lake and minimum distance from the lake to the moraine crest, only possible to extract from high resolution DEMs, we employ a simpler method. We use instead the mean slope of the lake front area to represent the steepness of the moraine.

First, a slope raster file is generated from the DEM. The dimensions of the lake front area are set by treating the existing lake outlet as the midpoint and drawing an area with a radius of 100 m (Figure 4). The mean slope of this area is calculated with the help of the slope raster. A radius of 100 m is chosen based on a previous maximum breach width of the test lake – 200 m (Vuichard & Zimmermann, 1987). Here, we note that the breach width is related to the moraine composition and its material properties (Shrestha et al. 2010). As the type of material the moraine is composed of is difficult to distinguish from satellite imagery, we use a lake breach width from an event in the same region.

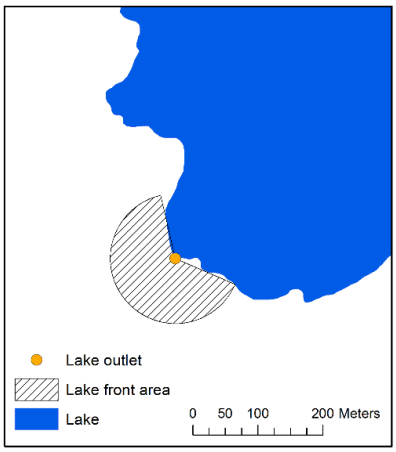

Figure 4. Lake front area drawing example. The lake outlet point is taken as the area center. Source: Glacier and Glacial Lake Inventory of Bhutan using ALOS Data (Version 16.11), JAXA.

To consider the likelihood of glacier calving, sudden release of glacial drainage or the occurrence of ice avalanches into the lake, the following indicators are selected:

Distance to parent glacier: Lakes within a distance of 500 m from the parent glacier are further considered as potentially hazardous (Cook et al. 2016; Wang et al. 2015). The distance between the lake and the lowest point of glacier terminus closest to the lake boundary is found.

Glacier end mean slope: Parent glacier end or snout steepness was estimated. Bolch et al. (2011) use a surface steepness threshold of 25 degrees for probability of ice avalanches. Figure 5 shows how the glacier end area was defined. The lowest point of the glacier closest to the lake was saved as a point feature class and an area with radius 500 m from the point was drawn through the buffer tool. The resulting area was intersected with glacier area to get the lowest 500 m of the lake associated glacier area. The mean slope was calculated for this area as an estimate of its steepness.

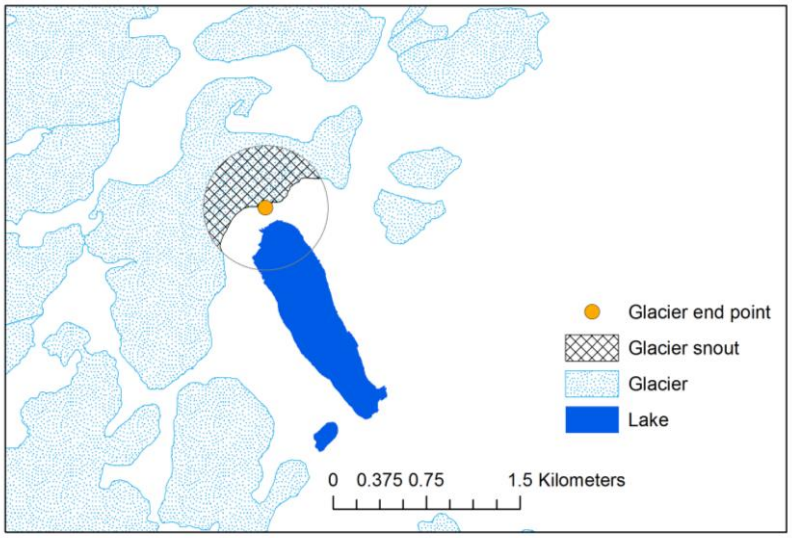

Figure 5. Hatched area shows the glacier snout area used to calculate mean slope. Radius is 500 m. Source: Glacier and Glacial Lake Inventory of Bhutan using ALOS Data (Version 16.11), JAXA.

Data processing procedures for hazard indicators explained above are carried out in ArcGIS as shown in Figure 6. Hazard classes from Table 4 are applied to the outputs – lake size, distance from glacier, mean slope of lake front area, mean slope of glacier end.

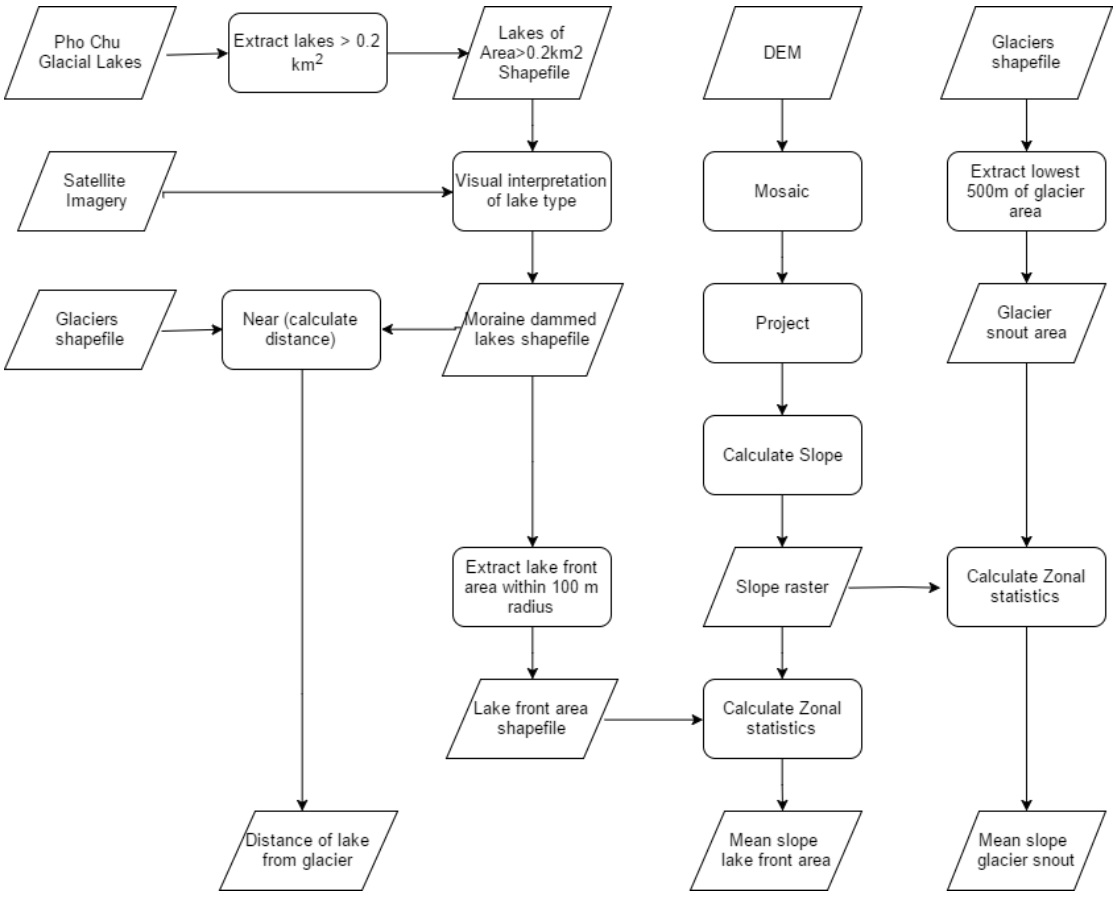

Figure 6. Process summary for implementing lake hazard assessment with ArcGIS. The ASTER GDEM tiles, downloaded from USGS, were merged and projected to WGS 1984 UTM Zone 46N for the area covering Bhutan. A slope file was generated from the DEM. Lakes greater than 0.2 km^2 were selected and further subset according to lake type. The shortest *distance between the lake's boundary and associated glacier* was found using the glacier end point. The *mean slope of lake front area* was calculated using the lake front area and slope raster file. The *mean slope of glacier snout* was calculated using glacier snout area and slope raster file.

3.3 Flood modelling

A new dynamic overland flow model developed by Nilsson (2017), based on a Triangular Form based Multiple flow algorithm (TFM) (Pilesjö & Hasan 2014), is used to derive flood inundation maps for a lake outburst scenario (Section 3.3.3). Such a hydrological model has not been used before in a glacial lake hazard context.

The model is flexible with respect to inputs of spatially varying values of precipitation, friction and infiltration. In case of remote mountain regions where field work is quite labor intensive, the model can use freely available data such as the GDEM and give an indication of potential flood depths and velocity.

3.3.1 Model description

The principles behind the dynamic runoff model and the TFM algorithm are originally described in detail in Nilsson's (2017) thesis and Pilesjö & Hasan's (2014) paper. In this section, a brief overview of the dynamic model is described from Nilsson (2017).

The model is meant to be more comprehensive than past digital elevation based models which currently exist, such as the single flow or multiple flow, by additionally considering the time dimension and water depth. It is less complex than the physically based flood models which require many detailed parameter inputs. The model is run in a MATLAB environment.

The main input is a DEM over a fixed study area. Users can specify temporal and spatial variation of precipitation inputs in mm/hour. Flow can be modelled for the duration of flood or longer, while water depths at each time step are saved. Additional input matrices are infiltration (mm/h), surface roughness (n) or Manning's friction value, all represented by grid cell based data of the same resolution and geographic reference. There is flexibility for friction and infiltration values to vary spatially or be set to a constant.

During this model's development, Nilsson tested rainfall runoff distribution on high resolution elevation data covering urban and rural areas in Sweden. In this study, however, flow is modelled from a small source, a dam breach over mountainous terrain represented by a coarse resolution DEM (30 by 30 m). Instead of precipitation intensity, the input is flood intensity or discharge at the lake outlet or assumed moraine breach point.

The model saves water depths for each time step. Users can retrieve spatial distributions of water depths at specified minute instances as separate files. The maximum water depths reached at each cell are also saved.

The maximum flow velocities can also be saved as an output, as well as the water depths reached at maximum velocity. A note to make about the velocity output from the model is that it is a result of instantaneous velocity calculations, because a new velocity for each cell is calculated at every time step of incoming flows from immediate neighbor cells. This is different from the cumulative or resultant velocity of flows from upstream.

In one time step, the basic intermediate steps from Nilsson (2017), are as follows:

In each cell, the current water volume receives precipitation, which is added to it and allows infiltration, which is subtracted. The result is the *Volume-precipitation-infiltration* (VPI) value, which is used for further calculations.

Flow distribution matrices are generated for each focus cell with respect to the cell's immediate eight neighbor cells. The proportion of water each neighboring cell will receive from the focus cell is recorded in the matrix.

The flow distribution from the focus cell is based on the TFM algorithm (Pilesjö & Hasan 2014). The static TFM algorithm allows external routing to be carried out from each facet in the focus cell containing water to neighboring cells based on elevation differences between the facet and neighboring cell. A facet represents 1/8 of the focus cell and is defined as a plane in 3 dimensions with a constant slope and aspect derived from the focus cell and neighboring cells' elevation values. If one or more neighboring cells have a lower elevation, the flow is divided between them.

In the dynamic model, the flow distribution follows the same principle of divided flow. However, the slope is derived from surface elevation of water heights of the focus cell and neighboring cells. Surface elevation of water height is equal to the ground elevation added to the water height in the cell.

Assuming uniform open channel flow from one cell center to another, the model calculates velocity of flow by the Manning formula:

$$v = \frac{1}{n} R^{\frac{2}{3}} \beta^{\frac{1}{2}} \qquad (1)$$

where v is the average velocity (m/s) in the channel, n is the Manning surface friction value, R is the hydraulic radius (m), and β is the slope (m/m) (Ward & Elliot 1995). For the model, the hydraulic radius is defined with help of the difference between water surface elevations of neighboring cells or the water depth, whichever is smaller. R is the ratio of the cross-sectional area of a rectangular channel and the wetted perimeter. The slope is based on water surface elevation differences. The average velocity allows calculation of the distance water flows in one time step.

Volume of water flowing out of the focus cell (V_{out}) is then calculated. This quantity is mainly a function of the VPI, the flow distribution and the distance travelled in one time step.

Finally, the new water volume incorporates VPI, V_{out} or water leaving the cell, and incoming water volumes from eight neighbor cells.

3.3.2 Pilot area

Bhutan hosts a small population of 714,000 people as recorded in 2009 by the government, of which 66 percent reside in villages, as reported by the FAO country profile (2011). Highest population densities are found in lower elevations. Figure 7 shows the location of Bhutan, sharing a border with China in the north and with India

in the west and south. The country is mostly mountainous terrain, with peak elevations ranging between 7500 m and 200 m above sea level. The average yearly rainfall here is about 2000 mm. Ten percent of the country is covered by snow and glaciers and about 70 percent by forests (FAO 2011). The north hosts a harsh winter and short summer. During monsoon season, it is common to have heavy rains, flash floods and landslides (Fraser et al. 2001).

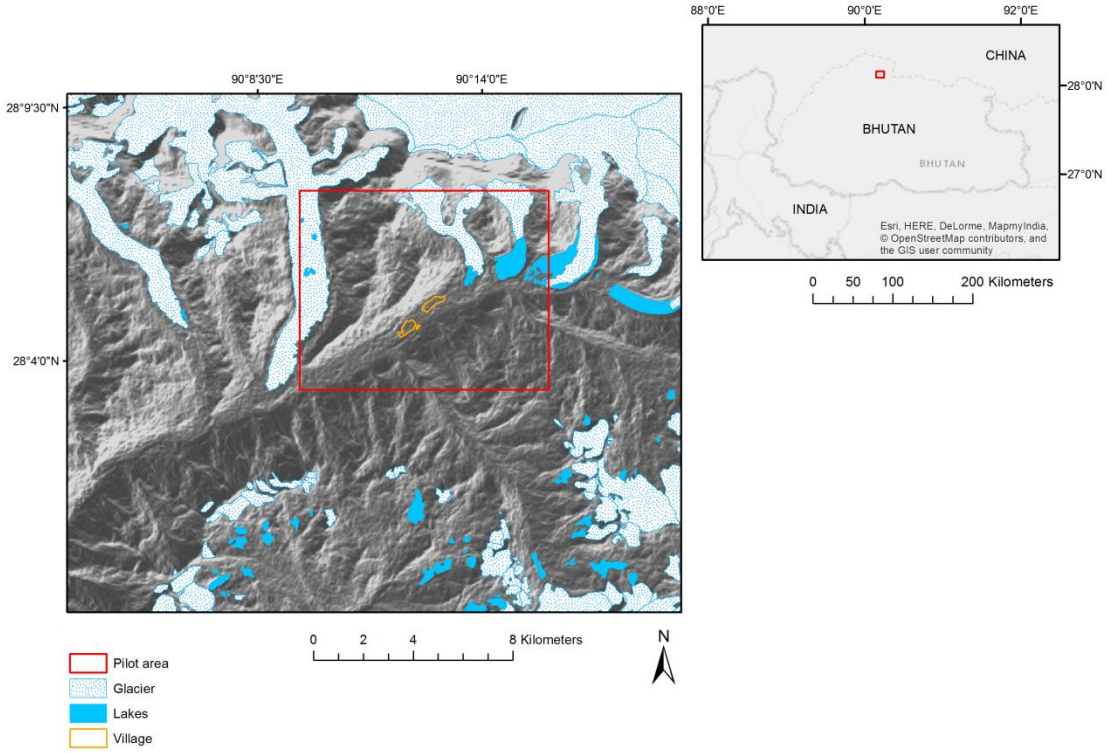

Figure 7. Pilot area (left) selected for flood modelling lies in the north-west Gasa district of Bhutan. Source: Glacier and Glacial Lake Inventory of Bhutan using ALOS Data (Version 16.11), JAXA. Background is a hill shade generated from ASTER GDEM v2. Source for map of Bhutan (right): ESRI, HERE, DeLorme, MapmyIndia, OSM, GIS user community.

In the north-west region of Bhutan, the Mo Chu and Pho Chu rivers, part of the 320 km Puna Tsang Chu river basin (9645 km^2) (State of the Environment Report 2016), originate from the Great Himalayan mountain range, flow towards Punakaha town and then towards India.

The pilot area for this study lies in Gasa district, in the northwest part of the country where the Pho Chu river emerges. The district is one with the least population, hosting 3,116 people. From statistics reported by Ministry of Agriculture, land use in Gasa consists of forest (33.3%), pasture (5.3%), agriculture (0.2%), others (rocky outcrops, perpetual snow) (61.7%) (Strategic Assessment Report 2009). Most glacial lakes in the basin cover an area ranging between 0.01 and 0.1 km^2, situated above altitudes of 4500 m (Veettil et al. 2016). Figure A1 in Appendix A shows a map of lakes and glaciers in the Pho Chu sub-basin in Bhutan.

Raphstreng lake emerged in the early 1950s as a supraglacial lake and is chosen as a potentially hazardous site for flood modelling. It lies at an approximate elevation of 4340 m, with a narrow moraine separating it from another glacial lake, Thorthormi, on its east side. The lake was chosen for flood modelling primarily due to its large area and remote location. Komori (2008) recorded the lake's area expansion between 1957 and 2001 as 0.028 km^2/year, with a lake area reaching 1.25 km^2 in 2001. It has turned into a moraine dammed lake, with a measured volume of 66,830,000 m^3 (Yao et al. 2012). During the years 1996-1998, the government carried out mitigation measures by digging a drainage outlet at the lake front to lower the water level. Two small settlements, Thanza and Dhamji, are located close by.

3.3.3 Model settings

Data preparation began with selecting the pilot area extent, as illustrated in Figure 8. The selected pilot area measures approximately 10.4 x 8.4 km and covers Raphstreng lake and two settlements downstream. Four tiles of GDEM were mosaicked and projected to WGS_1984 UTM zone 46N. The input elevation raster was prepared by clipping the DEM mosaic raster with the pilot area extent.

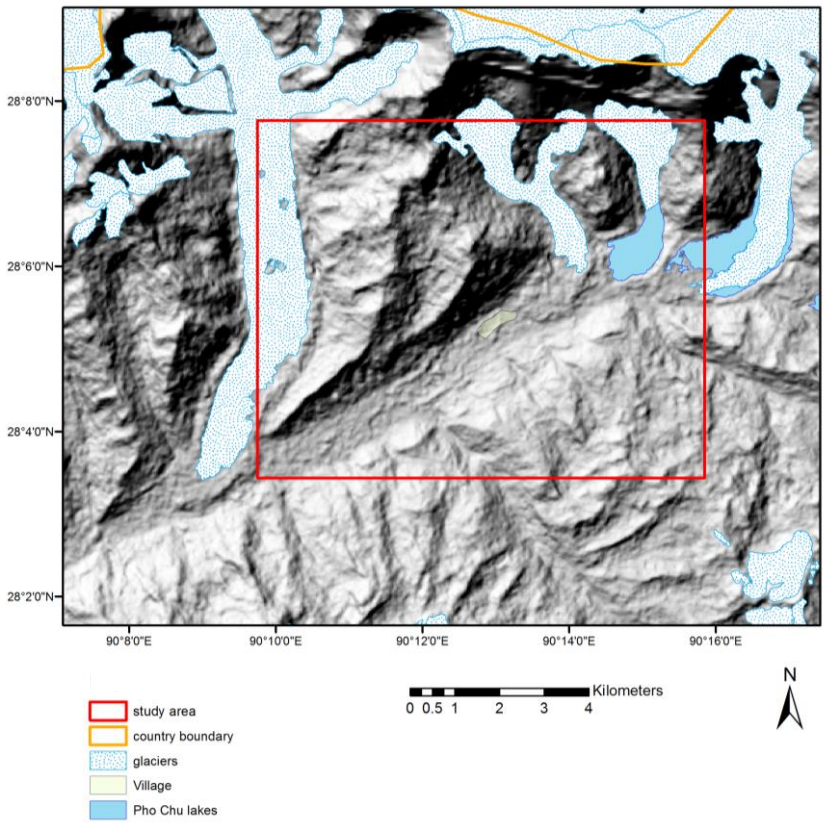

Figure 8. Model input extent for Raphstreng lake flood modelling, measuring approximately 10.4 x 8.4 km. Lakes from the left to right; Raphstreng, Thorthormi. The area is part of Gasa district, Bhutan. Source: Glacier and Glacial Lake Inventory of Bhutan using ALOS Data (Version 16.11), JAXA. The hill shade background is generated from ASTER GDEM V2.

Time varying flood discharge files are prepared for 25 minute intervals as shorter time intervals would require additional data preparation. For a 200 minute flood duration, preparing 8 files for discharge was reasonable given the time available for the study. Discharge values are estimated from a simulated hydrograph for a Himalayan lake where a peak discharge of 1700 m^3/s occurs at ~130 minutes (Figure 9). The hydrograph is taken to be an example of a glacial flood pattern from moraine collapse in the same region. The discharge files are prepared by setting the discharge values at the pilot lake front's estimated point of breach. Considering that the moraine breach width depends mostly on the moraine material, the breach width is estimated from the test lake's actual average breach width of 141 m, calculated from assuming a triangular breach shape (Vuichard and Zimmermann 1987). In the DEM, this is approximated to diagonally cover 3 cells in front of the lake. The discharge is divided over these 3 cells, changing values every 25 minutes. All raster files are converted to ASCII files for model input.

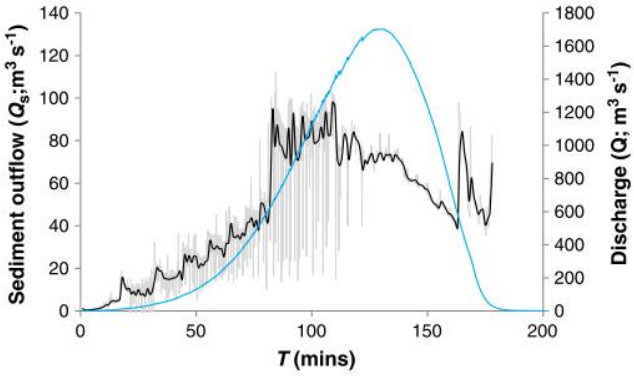

Figure 9. A simulation result from a reconstruction of a Himalayan lake burst event (1985 Dig Tsho lake, Nepal) at the moraine breach point used as a test example case. Such a hydrograph, a result from dam breach modelling, is often used as an input to glacial lake flood inundation models. The blue line represents the lake water flow rate (m^3/s). The black line shows the approximated volume rate of sediment released with the moraine breach expansion. Figure reprinted from Earth Science Reviews, 134 (2014), Westoby et al. (2014a), *Modelling outburst floods from moraine-dammed glacial lakes*, p 149, Copyright (2014), with permission from Elsevier.

Scaled input discharge values for Raphstreng lake are shown in Table 5. Compared to the test case lake modelled in Figure 9, Raphstreng's lake volume is much higher. To determine the amount of drainage of Raphstreng lake, we assume a linear relationship between percentage drainage of lake's water volume and moraine steepness. The discharge values from the test case are scaled by a factor derived from the assumed linear relationship between these two variables. For the test case, the moraine steepness before the outburst was reported to be between 25 and 30 degrees and the lake was reported to be completely drained (Vuichard and Zimmermann 1987). We use a value of 27.5 degrees related to 100% lake drainage to obtain a scale factor. For Raphstreng lake, the result from the DEM yields a mean slope of 8.62 degrees (Table 7b, Section 4.1). When scaled for percentage drainage with respect to slope, Raphstreng lake is estimated to drain 31%, equal to a total release of 20,948,167 m^3 of water.

Table 5. Input flood discharge values for Raphstreng lake, assuming 31% lake drainage over 200 minutes, scaled from a test lake burst hydrograph in the same region (Westoby et al. 2014a). Maximum discharge of 4,926 m/s occurs at 125 minutes. The input is converted to mm/hr for 30 x 30 m cell size. It is divided over 3 cells, to approximately represent the test lake's average breach width at the lake outlet. The discretized values at 25 minute intervals from Figure 9 are used as multiple inputs to the dynamic flood model at the lake outlet.

Time (min)	Scaled Discharge (m^3/s)	Discharge for 900 m^2 cell area (mm/hr)	Discharge per cell (mm/hr)
0	0	0	0
25	58	231,792	77,264
50	435	1,738,437	579,479
75	1,449	5,794,790	1,931,597
100	3,332	13,328,018	4,442,673
125	4,926	19,702,287	6,567,429
150	3,477	13,907,497	4,635,832
175	290	1,158,958	386,319
200	0	0	0

Further settings for the model include the Manning friction value (n), which is assumed to be 0.035 for stony earth channels with cobbles, as well as farmland on floodplains (Chow 1959). Infiltration is assumed to be a spatially constant value of 20 mm/h for sandy loam soil type (FAO 1990b). It was found from a geological survey study in Bhutan that a soil sample above 4000 m elevation consisted of mostly alpine turf soils and un-weathered glacial deposits, otherwise classified as *Regosols*, weakly developed soils. The top soil layer is described as fine sandy loam, with few quartz and slate gravel (Baillie et al. 2004).

The flood duration is set to 200 minutes as approximated from Figure 9 and post flood modelling time is set to 100 minutes. The post flood modelling time is kept to observe the duration of water level inundation in the study area after the lake has drained to its limit.

A time step of 0.25 seconds was set to satisfy the velocity condition of the model which ensures model stability. After several trial runs of using different time steps, the highest time step was chosen which did not violate the velocity condition. If a higher time step, such as 0.5 seconds had been chosen, the distance calculated for flow in one time step would have exceeded the neighboring cell dimensions after a few iterations. A lower time step was possible but would require more iterations and thus higher model run time.

3.4 Vulnerability

This section is limited to the physical aspect of vulnerability alone, excluding economic, environmental and social aspects. Here, physical vulnerability is assumed to be measurable in terms of *the degree of hazard coinciding with settlement areas*. Water depth and velocity of the flow is used to define physical vulnerability through a semi-quantitative rating.

The degree of hazard is calculated using the formula and flood hazard classes as developed by Ramsbottom et al. (2006) for development planning guidance for the UK Environment Agency. These classes are defined in terms of the level of danger to a person who can drown or be swept over by flowing water. The thresholds are set by the authors on the premise that most people will not be able to stand when flood depth is 0.6 m and velocity of flow is 2 m/s.

$$HR = d*(v+0.5) + DF \qquad (2)$$

where HR is the hazard rating (m^2/s), *d* is the water depth (m), *v* is the flow velocity (m/s) and *DF* is the debris factor. The *DF* can be set to 1, 0.5 or 0 depending on land use. A DF of 0.5 is chosen which is recommended for depths greater than 0.75 m, as most of the inundated extent is greater than this value from the modelling result (section 3.7). Table 6 shows the intervals and class descriptions for ranking degree of hazard.

Table 6. Hazard Rating (HR) classes and description adapted from Ramsbottom et al. (2006).

Hazard Rating (HR)	Hazard category	Description
< 0.75	Low	Caution Flood zone with shallow flowing water or deep standing water
0.75 - 1.5	Moderate	Dangerous for some (i.e. children) Flood zone with deep or fast flowing water
1.5 - 2.5	Significant	Dangerous for most people Flood zone with deep fast flowing water
> 2.5	Extreme	Extremely Dangerous for all Flood zone with deep fast flowing water

Using the results from flood modelling (Section 4.2), maps of maximum velocity and depths at maximum velocity are combined using equation 2 to obtain the hazard map. The result is then overlaid with settlement areas to identify hazard degree to human settlements. Google Earth imagery was used to digitize settlements in the pilot area near the lakes.

We also attempt to classify magnitude of hazard by only considering the flood depth, by assigning moderate and higher degrees of hazard for depths more than 1 m.

3.5 Limitations and assumptions

In this study, dam breach modelling has not been carried out. Instead, the hydrograph at the breach point is assumed from a previous dam breach model result of a lake from the same region. The input hydrograph is adjusted for Raphstreng lake under certain assumptions as explained in Section 3.3.3.

Sediment is an important factor in mountain catchments and has an effect on the nature of flow. Glacial flood flow can become concentrated with mud, logs and debris with time, but sediment erosion and transport could not be considered while modeling flood runoff in this study.

4 Results

4.1 Hazardous assessment results

In the Pho Chu river sub basin, there are 37 lakes with an area greater than 0.1 km^2 out of 142 lakes recorded in the ALOS dataset, and 14 lakes were found with area greater than 0.2 km^2. Table 7a lists lakes with area greater than 0.2 km^2 and lake type. Six lakes were determined to be dammed by moraines. The remaining were clearly supraglacial or moraines could not be determined from the image. Table 7b lists only moraine dammed lakes with their hazard indicator calculations.

Thorthormi lake has another lake of size 0.33 km^2 area next to it, which is also in contact with the parent glacier, along with other smaller supraglacial lakes. It has a lateral moraine separating it from Raphstreng Lake.

Table 7a. Lakes of area greater than 0.2 km^2, in the Pho Chu sub-basin, Bhutan and type determined from satellite imagery. Other attributes are listed from the glacier lake dataset.

MAP_ID	Type of lake (Supraglacial =SG; Moraine dammed = MD)	AREA (km^2)	Elevation (m)	Longitude	Latitude
Ph-008	Unclear	0.712	5002	89° 55' 47.897" E	27° 56' 28.291" N
Ph-016	Unclear	0.640	5078	89° 55' 48.512" E	27° 58' 24.095" N
Ph-025	MD	0.252	4268	89° 53' 54.979" E	28° 6' 21.791" N
Ph-027	MD	0.439	4341	89° 54' 33.607" E	28° 6' 50.377" N
Ph-037	MD	0.348	4690	90° 1' 40.211" E	28° 6' 46.608" N
Ph-050 (Raphstreng Lake)	MD	1.226	4339	90° 14' 50.091" E	28° 6' 23.432" N
Ph-051 (Thorthormi Lake)	SG and MD	1.172	4453	90° 15' 55.917" E	28° 6' 24.738" N
Ph-057 (Luggye Tsho)	MD	1.360	4510	90° 18' 0.086" E	28° 5' 33.842" N
Ph-072	SG	0.465	5329	90° 17' 20.740" E	27° 59' 47.621" N
Ph-091	unclear	0.527	5132	90° 12' 38.140" E	28° 0' 57.384" N
Ph-096	unclear	0.234	4939	90° 13' 19.114" E	27° 59' 43.562" N
Ph-100	unclear	0.675	5078	90° 13' 58.360" E	27° 58' 40.885" N
Ph-117	SG	0.241	5146	90° 15' 45.006" E	27° 55' 11.872" N
Ph-126	SG	0.416	4918	90° 12' 25.674" E	27° 52' 33.135" N

Table 7b. Moraine dammed lakes in the Pho Chu sub-basin, Bhutan and their indicator calculations. *Thorthormi lake has other subglacial lakes surrounding it, one which is 0.33 km^2 in area.

MAP_ID	AREA (km^2)	Distance from glacier if < 500 m	Mean Slope of glacier end (500 m) (degrees)	Standard deviation of glacier end slope	Mean slope of lake front area (degrees)	Standard deviation of mean slope
Ph-025	0.252	261	21.85	11.67	9.75	3.56
Ph-027	0.439	275	28.44	9.77	22.94	4.14
Ph-037	0.348	0	14.44	6.23	5.90	2.93
Ph-050 (Raphstreng)	1.226	0	12.77	7.35	8.62	2.98
Ph-051 (Thorthormi)*	1.172	0	27.17	17.81	8.41	3.78
Ph-057 (Luggye)	1.360	0	11.05	5.73	13.11	6.75

The results show 6 moraine dammed lakes in the Pho Chu basin of area greater than 0.2 km^2 and 6 of them classified as potentially hazardous by at least one indicator (Table 7b). For all 6 lakes, the distance from associated glacier is less than 500 m. Lake Ph-027 and Ph-051 have mean glacier end slopes greater than 25 degrees. Four lakes have mean slopes of lake front area falling in the moderate hazard potential class. Lake Ph-027 has the highest mean slope of lake front area, falling in the high hazard potential class. Lake Ph-057 has the greatest surface area of 1.36 km^2. Lake Ph-051, or Thorthormi lake, has the greatest lake perimeter in contact with its parent glacier.

Lake Ph-008 could be hazardous as it rests on a high elevation and steep slope, though it is not clear if it is moraine dammed. Lake Ph-016, also of considerable size, rests on a very high elevation and has a steep drop.

4.2 Flood modelling results

The model iterations ran for about 10 hours on a standard laptop for total flood and post flood time of 300 minutes. Water depths were recorded in meters for every time step. Snapshots of water depth extents at different times are attached in Appendix B (Figures B1 - B6).

Figure 10a shows the maximum water depth reached in the pilot area during 300 minutes. The maximum flood depths mostly fall between 1 to 15 m (Figure 10b). Spatially concentrated in the main river channel, the flood extent entered the first settlement area at about 140 minutes from the start time, and after 180 minutes the settlement was completely inundated. The greatest water depths were found to be in the existing stream channel – first immediately near the source, then right before the channel narrows and at a sharp depression occurring after the second settlement.

At 300 minutes, water had not left the settlement areas, though had traveled further downstream about 6.4 km away from the source. The total inundated area was 2.9 km^2.

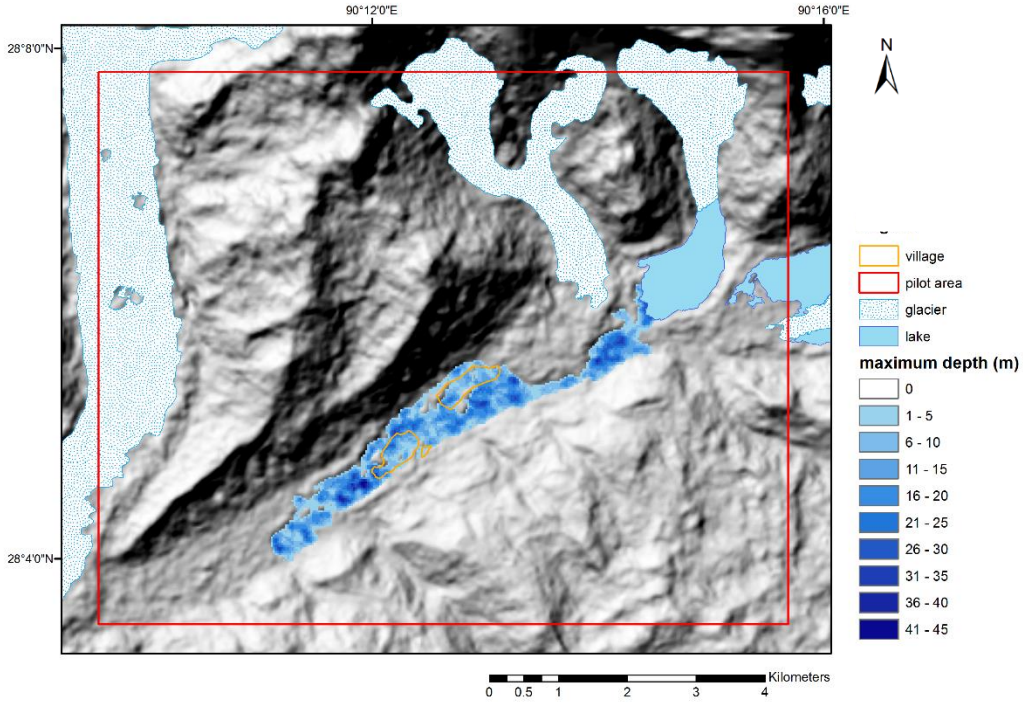

Figure 10a. Maximum water depths reached during the dynamic model run within total time of 300 minutes (200 minutes for flood duration and 100 minutes post flood), recorded in meters. Model run time is ~10 hours on a standard laptop. The background is a hillshade generated from the ASTER GDEM v2. The total flooded extent covers about 2.9 km^2, including a majority of the settlement areas. Source: Glacier and Glacial Lake Inventory of Bhutan using ALOS Data (Version 16.11), JAXA. The hill shade background is generated from ASTER GDEM V2.

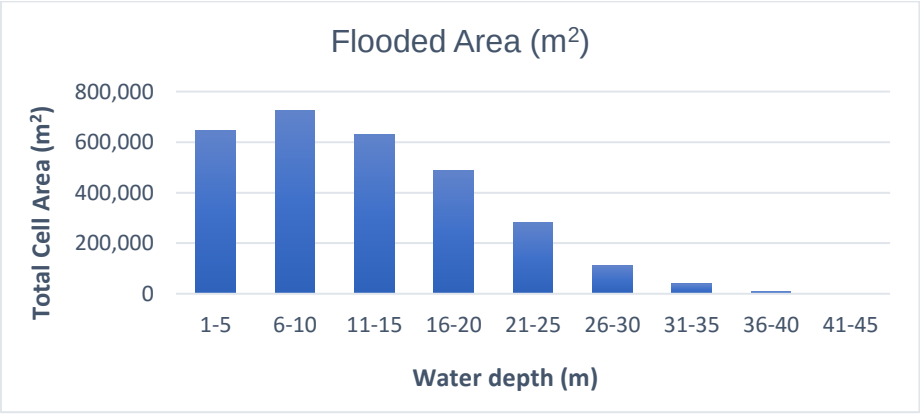

Figure 10b. Flooded area and maximum water depth distribution reached during 300 minutes of flood modelling time.

Figure 11 shows the result of maximum velocity reached during the flooding event. The maximum velocity reached up to 35 m/s. The highest velocities were observed near the source at the moraine, up to 23 m/s and again through the narrow channel, reaching 35 m/s. After this, the velocity then mostly remains between 6 and 10 m/s.

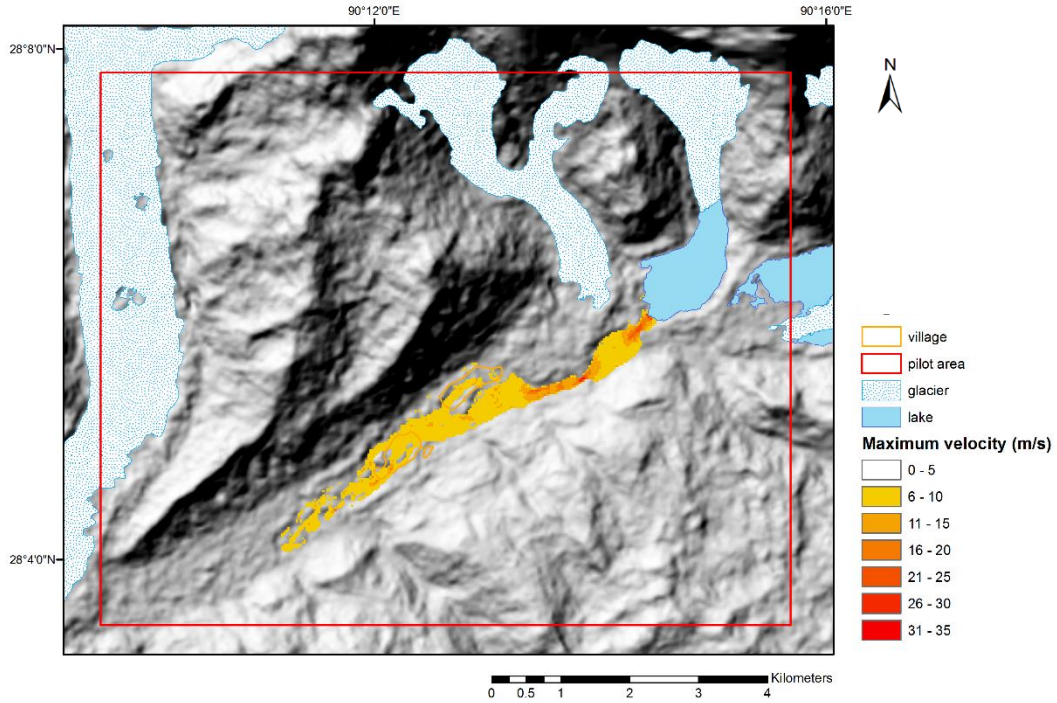

Figure 11. Maximum velocity (m/s) result from the TFM dynamic model, reached at each cell of the pilot area during 300 minutes. The flow velocity is calculated by the Manning formula for uniform open channel flow. The output shows the instantaneous average velocity recorded in a single time step for each cell and does not show the resultant velocity of flow from the source. Source: Glacier and Glacial Lake Inventory of Bhutan using ALOS Data (Version 16.11), JAXA. The hill shade background is generated from ASTER GDEM V2.

The depths obtained at maximum velocity are up to 37.5 m (Figure 12). Highest velocity recorded in the settlement area is 11 m/s and 15 m/s in the second settlement.

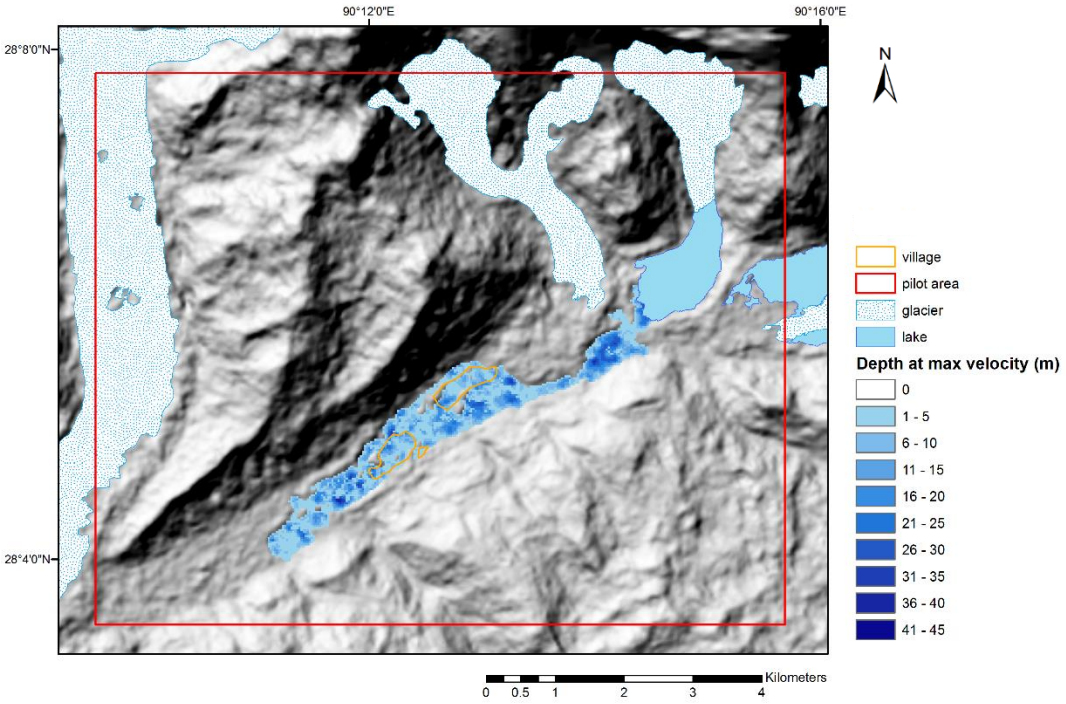

Figure 12. Water depths in meters at maximum velocity, a result from the TFM dynamic model. Source: Glacier and Glacial Lake Inventory of Bhutan using ALOS Data (Version 16.11), JAXA. The hill shade background is generated from ASTER GDEM V2.

4.3 Vulnerability

Figure 13 shows the result of mapping hazard magnitude using Ramsbottom et al. (2006) hazard rating, which is a product of water depth and velocity. Figure 14 shows the hazard magnitude result classified only according to maximum flood depth in meters. Both results show that most of the inundated extent fell under the greatest hazard category. Almost all of the settlement areas were affected by the flood.

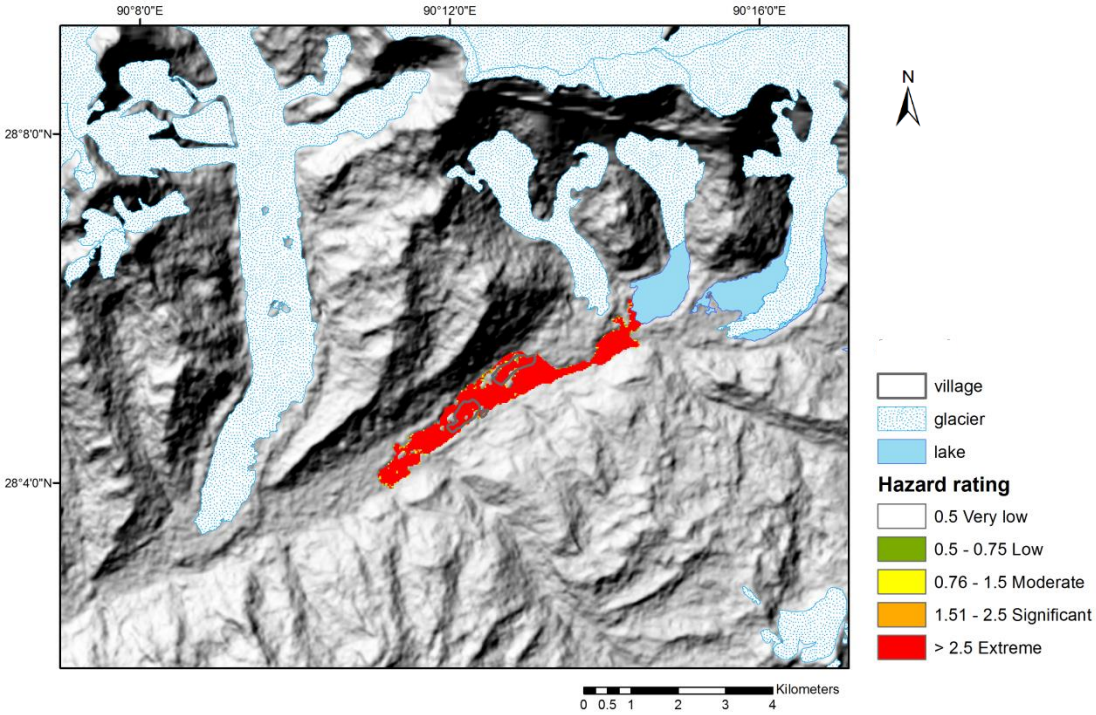

Figure 13. Degree of hazard classification by HR method using results of flow velocity and depth at maximum velocity from the TFM dynamic model. Source: Glacier and Glacial Lake Inventory of Bhutan using ALOS Data (Version 16.11), JAXA. The hill shade background is generated from ASTER GDEM V2.

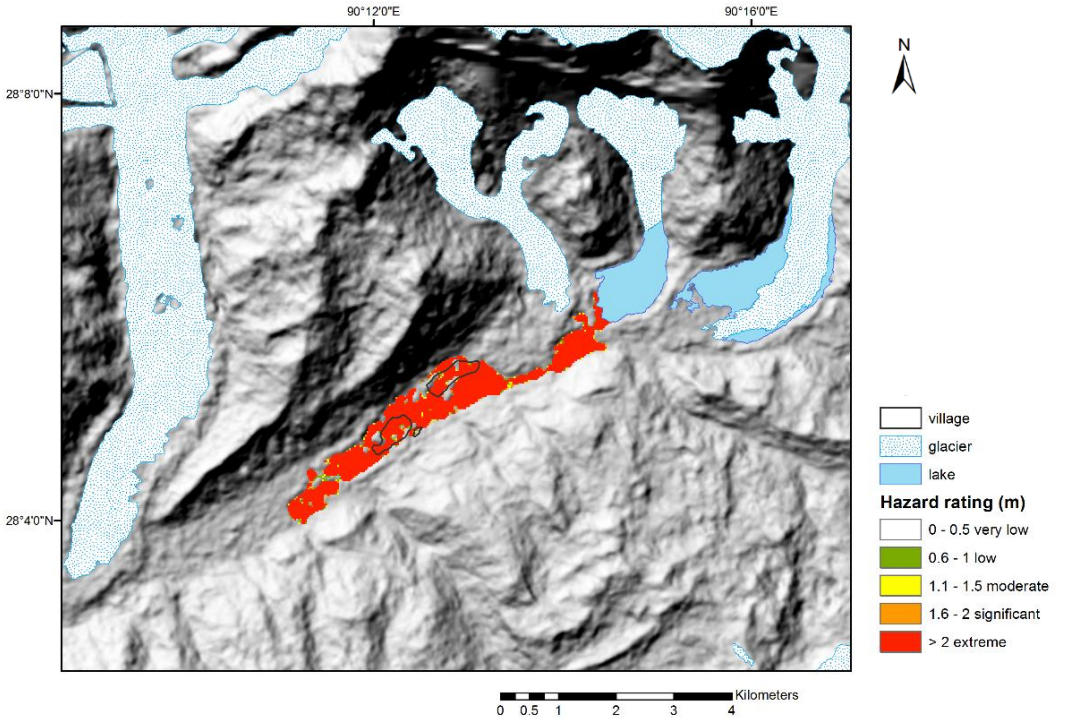

Figure 14. Degree of hazard classification using results of maximum water depth (m) from the TFM dynamic model. Source: Glacier and Glacial Lake Inventory of Bhutan using ALOS Data (Version 16.11), JAXA. The hill shade background is generated from ASTER GDEM V2.

5 Discussion

As each glacial lake and region has its own unique geographical characteristics, the study has attempted to generalize an extremely complex phenomenon in a simple way. The proposed framework can be evaluated in terms of the accuracy and simplicity of procedures, and the time taken to carry them out while incorporating major contributing factors. Further suggestions for improvement are discussed.

5.1 Hazard indicators

The geomorphological hazard indicators used for this assessment were selected on the basis of literature review and focused on the most crucial factors contributing to hazard potential. They were narrowed down using a criteria (section 4.2) which would allow a first stage assessment of glacial lakes without requiring a long term study and difficult data requirements.

It was possible with the available DEM to further include a slope analysis in the assessment for the likelihood of rock fall. Calculating the slope around the lake, would have given an indication for rock fall into the lake, similar to analyzing the glacier end slope for likelihood of ice avalanches. This is suggested to be included in the list of hazard indicators. The possibility of including it in this study was found out too late.

Selecting thresholds in the assessment could be slightly subjective, such as the limit used for lake area, as different studies have used varying thresholds. A better approach to selecting thresholds could be applied if sufficient data on lakes were consolidated and analyzed.

Factors that were not considered were the presence of permafrost near the moraine and seismic activity. Besides geomorphological features, Allen et al. (2008) have used permafrost distribution as an indication to buried ice presence in the moraine. The drawback to including this is that it would not always be possible to get a permafrost distribution map for all regions worldwide. Also, Bhutan has recorded 19 major earthquakes since 1713 (Osti et al. 2013). While previous seismic activity in the area can be considered, this would be better incorporated in a probabilistic approach (section 5.1.2).

Intense rainfall or snowmelt could lead to a rise in water level and lake overflow or moraine collapse (Emmer & Cochachin 2013). A low freeboard would be a better indicator to include this aspect and is suggested to be included when a higher resolution DEM is used. Rainfall and temperature patterns, however, could provide useful insight into external trigger causes.

It was realized that categorizing lake type was not always possible from satellite imagery. Previous field studies or knowledge about the geological characteristics of the glacial environment are useful and help to identify moraines and moraine types.

5.1.1 Moraine steepness

There could be different ways to determine the lake front area used to calculate the moraine steepness, and several spatial methods were attempted. The width-to-height ratio of the moraine is a crucial factor, but the possibility of measuring moraine dimensions depends on DEM resolution. The mean slope calculation is only suitable for the assessment if a finer resolution DEM is not available and when the height and width cannot be determined. A more accurate but more time consuming method would have been to determine the dam crest width from the lake shore and begin measuring the moraine steepness from the point of moraine descent. This would be possible in higher resolution DEMs as the dam crest could be as narrow as 30 m or as wide as 200 m, and would require visual interpretation of the area around each lake. In some cases, the lake boundary was highly irregular, especially in the case of Thorthormi lake, as it is surrounded by other smaller supraglacial ponds. For lakes of this type, the mean slope might be less accurate.

Finally, the mean slope of the lake front area rather than the steepest path from the lake was used. This method was selected so that the same process can be applied to all lakes. We conclude that calculating a mean slope for a fixed radius is better if many lakes are in the assessment area, but the method might give very low values for dams with greater crest width.

5.1.2 Hazard potential probability index

The assessment could be improved if weights were assigned to the hazard indicators using data from past events. Previous studies have assigned different weights for different regions. To arrive at a metric which is applicable to all moraine dammed lakes would require an in depth analysis of past events' data grouped by region. Instead of using thresholds for every indicator, indicator values could directly be used in calculating a probability index. In general, if the hazard potential depended on a number of indicators, it could calculated by

$$HP = \sum_{i=1}^{n} w_i I_i$$

where *HP* is the hazard potential, *w* is statistically derived weight, *I* is the hazard indicator such as moraine steepness or lake area and *n* is the number of hazard indicators.

5.2 Comparison of hazard assessment results

The first stage assessment showed 6 hazardous lakes in the Pho Chu basin, following the proposed criteria. Two of these lakes have already drained in the past - Luggye Tsho in 1994 and Tarina Tsho in 1957. Findings by Mool et al. (2001) showed 8 lakes classified as potentially hazardous in the Pho Chu sub-basin. However, the authors have used a different assessment methodology and have considered supraglacial lakes as well. Five of the moraine dammed lakes classified as potentially hazardous by Mool et al. (2001) have been also found by this assessment.

5.3 Using the TFM dynamic model in a hazard context

The dynamic model gives estimates for flow depth, flood extent and maximum flow velocity. The model is easy to run as it uses accessible data and can eventually help estimate the magnitude of hazard for glacial floods or dam break floods. Time taken for the model to run was reduced because the model performs the iterations only over cells which contain water.

A useful aspect of implementing the dynamic model in the future is that analysis of flood arrival time with respect to different settlements and infrastructure can be carried out, as water depths are saved for each time step. This information may be important for planning early warning systems for flood hazard. As the vulnerability result was derived from the model output, it is possible to add it as an additional output of the TFM dynamic model.

The model result of maximum velocity showed the instantaneous average velocity at every time step. We can infer that the result is then an underestimation of the actual velocity in case of a flood of same magnitude. Incorporating the conservation of momentum of flow would improve the model for the purpose of estimating hazard degree.

As we did not consider flow obstruction from mobilized sediment or vegetation during flood routing, the model results are better treated as estimates rather than absolute values, giving an indication of where and how much flood might impact an area.

The infiltration used for flood modelling (section 4.3.3) was a constant value for each cell, even though it was possible to use spatially varying infiltration in the model. The result can be improved with better knowledge of soil type and impervious surfaces in the pilot area.

5.4 Peak discharge and hydrograph

The hydrograph from Figure 5 was adjusted for Raphstreng Lake assuming a simple linear relationship between moraine steepness and the proportion of drained lake volume. There may be other approaches to determine how much water a lake can release. Peak discharge has been estimated using the volume-discharge empirical relationship derived from lakes in the Swiss Alps (Huggel et al. 2002),

$$Q_{max} = 0.00077\ V^{1.017} \qquad r^2 = 0.94 \qquad (3)$$

However, the above relation is more applicable when assuming a worst case scenario of complete lake drainage. In reality, the flood volume may be more or less, depending on the type of trigger mechanism.

5.5 Comparing model results

It is difficult to obtain data for validating a glacial flood model result. However, we can use a past recorded flood hydrograph which flowed through the same sub-basin from a lake burst close to Raphstreng lake. The hydrograph reading was recorded 100 km downstream from Luggye Tsho lake outburst in 1994. It released an estimated water volume of 48 million m^3 and levels rose up to 4 m at the station (Richardson & Reynolds 2000). The highest estimated velocity was 12 km/hr (Rothacher and Watanbe 1996). At Raphstreng lake, the modelled volume released was nearly half of Luggye Tsho, the average maximum water depth was 12 m within approximately 6 km from the source. We can speculate that the flood depth will reduce as it travels further downstream as described in Section 2.2 (Cenderelli & Wohl 2001).

Other model results of glacial lake flood runoff in mountain catchments have given inundation values up to 50 m (W. Wang et al. 2012) and 10 m (Khanal et al. 2015) using the HEC-RAS hydraulic model. The comparison cannot be easily made as there are many different variables involved. These include, but are not limited to, the resolution and quality of DEM, input hydrograph, channel width, infiltration and friction values. Osti et al. (2013) have modelled flood inundation in the Pho Chu sub basin, but with different initial conditions of peak discharge.

5.6 Data quality

Delineation methods of glacier and lake outlines are described in detail in Ukita et al. (2001) and Tandono et al. (2012). The authors report a root mean square error of 11.7 m for polygons. This might affect the result of distance calculations between lake and glaciers, but not the hazard category. With regard to DEM quality, the ASTER validation report (2011) states an overall accuracy of 17 m at the 95% confidence level for version 2.

5.7 Recommendations and future research

For further research, the relationship between moraine steepness and volume of previously drained lakes could be interesting to investigate. This would require systematic data compilation on glacial lakes. Though a global glacier outlines database exists (GLIMS), a global database for glacial lakes is still under development (Vilímek et al. 2014). For better model comparisons, such a database would greatly facilitate statistical analysis and provide a source for model validations. This should include yearly glacier and glacial lake outlines.

Another direction future analysis can take is in depth slope stability study, which involves studying material on inclined surfaces and their resistance to collapse or sliding. Sediments which are likely to slide can be studied with respect to their critical angles of repose – the maximum angle from the horizontal on which they can rest without sliding. This can help specify hazardous zones around the lake, from triggers such as rock fall, ice or snow avalanches. Rainfall and temperature patterns can be tested for significance with respect to such events in the past.

The dynamic model can be used to estimate hazard magnitude for different glacial lake flood scenarios, but validation of the model was not possible in this case. Where flood data are available from post-flood field surveys, the model can be validated, and model performance compared with other flood routing models.

6 Conclusion

While other assessments exist to identify hazardous lakes and downstream flood magnitude, this study introduces a new dynamic model for flood runoff, which is more comprehensive than single flow or multiple flow GIS based models and can be applied in any region. It can handle time varying discharge and spatially varying infiltration and friction values. A first stage assessment method applying GIS techniques is proposed for conditions where field work is not feasible and data are limited.

The hazard assessment framework could be useful to policy makers and disaster risk reduction professionals who are working in managing natural hazard and risk in mountain regions.

7 References

Alaska Satellite Facility. 2017. Retrieved 23 May 2017, from. https://www.asf.alaska.edu/blog/what-is-glacial-calving/

Aggarwal, A. et al. 2013. Glacial lake outburst flood risk assessment using combined approaches of remote sensing, GIS and dam break modelling. *Geomatics, Natural Hazards and Risk*, 7:18–36.

Allen, S., I. Owens, & P. Sirguey. 2008. Satellite remote sensing procedures for glacial terrain analyses and hazard assessment in the Aoraki Mount Cook region, New Zealand. *New Zealand Journal of Geology and Geophysics*, 51(1): 73–87.

Anon, 2016. Description of Glacier and Glacial Lake Inventory of Bhutan using ALOS (Daichi) Data (Version 16.11). Japan Aerospace Exploration Agency (JAXA) Earth Research Observation Center.

Baillie, I. C., K. Tshering, T. Dorji, H. B. Tamang, T. Dorji, C. Norbu, A. A. Hutcheon, and R. Baumler. 2004. Regolith and soils in Bhutan, Eastern Himalayas. *European Journal of Soil Science*, 55: 9–27.

Benn D.I., and D. A. Evans. 2010. Glaciers and Glaciation. Second edition. London, Hodder Education.

Bhutan State of the Environment Report, 2016. http://www.switch-asia.eu/fileadmin/user_upload/RPSC/country-level-work/Bhutan/Bhutan-State-of-Environment-Report-2016.pdf

Jain S. K., A. K. Lohani and R. D. Singh. 2015. Identification of Glacial Lake and the Potentially Dangerous Glacial Lake in the Himalayan Basin. In *Dynamics of Climate Change and Water Resources of Northwestern Himalaya*, eds. R. Joshi et al., pp.85–96. Springer International Publishing Switzerland.

Bolch, T. et al., 2011. Identification of potentially dangerous glacial lakes in the northern Tien Shan. *Natural Hazards*, 59: 1691–1714.

Casassa, G., J. Rodriguez, & T. Loriaux. 2014. *Global Land Ice Measurements from Space*.

Cenderelli, D.A., & E.E. Wohl. 2001. Peak discharge estimates of glacial-lake outburst floods and “normal” climatic floods in the Mount Everest region, Nepal. *Geomorphology*, 40: 57–90.

Che T., L. Xiao & Y. Liou. 2014. Changes in Glaciers and Glacial Lakes and the Identification of Dangerous Glacial Lakes in the Pumqu River Basin,

Xizang (Tibet). *Advances in Meteorology*, vol. 2014, Article ID 903709, 8 pages.

Chow V.T. 1959. *Open-channel hydraulics*. New York. McGraw-Hill.

Clague, J.J. and S.G. Evans. 2000. A review of catastrophic drainage of moraine-dammed lakes in British Columbia. *Quaternary Science Reviews.* 19: 1763–1783.

Cook, S., I. Kougkoulos, L. Edwards, J. Dortch, and D. Hoffmann. 2016. Glacier change and glacial lake outburst flood risk in the Bolivian Andes. *The Cryosphere* 10: 2399-2413.

Emmer, A. & A. Cochachin. 2013. The causes and mechanisms of moraine-dammed lake failures in the cordillera blanca, North American Cordillera, and Himalayas. *Acta Universitatis Carolinae, Geographica*, 48: 5–15.

FAO Country Profile, 2011. http://www.fao.org/nr/water/aquastat/countries_regions/Profile_segments/BTN-GeoPop_eng.stm

FAO**,** 1990. *Irrigation water management: irrigation methods,* Training manual No. 5 (Provisional edition) C. Brouwer, K. Prins, M. Kay & M. Heibloem. Rome. http://www.fao.org/docrep/S8684E/s8684e0a.htm

Fraser, N., A. Bhattacharya, & B. Bhattacharya. 2001. *Geography of a Himalayan Kingdom: Bhutan*. New Delhi. Concept Publishing Company.

Frey, H. et al. 2016. A robust debris-flow and GLOF risk management strategy for a data-scarce catchment in Santa Teresa, Peru. *Landslides*, 13: 1493.

Fujita, K., A. Sakai, S. Takenaka, T. Nuimura, A. Surazakov, T. Sawagaki, and T. Yamanokuchi. 2013. Potential flood volume of Himalayan glacial lakes. *Natural Hazards and Earth System Science*, 13: 1827-1839.

Hubbard, B., A. Heald, J. Reynolds, D. Quincey, S. Richardson, M. Luyo, N. Portilla, and M. Hambrey. 2005. Impact of a rock avalanche on a moraine-dammed proglacial lake: Laguna Safuna Alta, Cordillera Blanca, Peru. *Earth Surface Processes and Landforms* 30: 1251-1264.

Huggel, C. et al. 2004. An assessment procedure for glacial hazards in the Swiss Alps. *Canada Geotech Journal*, 41:1068–1083.

Huggel, C. et al. 2002a. Assessment of Glacier Hazards and Glacier Runoff for Different Climate Scenarios Based on Remote Sensing Data : a Case Study for a Hydropower Plant in the Peruvian Andes. *EARSeL eProceedings*, 23: 22–33.

Huggel, C. et al. 2003. Regional-scale GIS-models for assessment of hazards from glacier lake outbursts: evaluation and application in the Swiss Alps.

Natural Hazards and Earth System Science, 3: 647–662.

Huggel, C. et al., 2002b. Remote sensing based assessment of hazards from glacier lake outbursts: a case study in the Swiss Alps. *Canadian Geotechnical Journal*, 39: 316–330.

Humanitarian Data Exchange. 2015. https://data.humdata.org/dataset/bhutan-settlements

ICIMOD, 2011. Glacial lakes and glacial lake outburst floods in Nepal. Kathmandu.

International Conference Report, 2012. Glacial lake outburst flood. 'Reducing Risks and Ensuring Preparedness'. Bhutan.

Iribarren Anacona, P., K.P. Norton, & A. Mackintosh. 2014. Moraine-dammed lake failures in Patagonia and assessment of outburst susceptibility in the Baker Basin. *Natural Hazards and Earth System Sciences*, 14: 3243–3259.

Iturrizaga, L., 2011. Glacier Lake Outburst Floods. In *Encyclopedia of Snow, Ice and Glaciers*, eds. V. P. Singh, P. Singh, & U. K. Haritashya, pp. 381–399. Dordrecht: Springer Netherlands.

Kattelmann, R. 2003. Glacial lake outburst floods in the Nepal Himalaya: A manageable hazard? *Natural Hazards*, 28: 145–154.

Khanal, N.R. et al., 2015. A comprehensive approach and methods for glacial lake outburst flood risk assessment, with examples from Nepal and the transboundary area. *International Journal of Water Resources Development*, 31: 219–237.

Komori, J. 2008. Recent expansions of glacial lakes in the Bhutan Himalayas. *Quaternary International*, 184: 177–186.

Masannat, Y.M. 1980. Development of piping erosion conditions in the Benson area, Arizona, U.S.A. *Quarterly Journal of Engineering Geology and Hydrogeology*, 13: 53-61.

McKillop, R.J. & J.J. Clague. 2007. Statistical, remote sensing-based approach for estimating the probability of catastrophic drainage from moraine-dammed lakes in southwestern British Columbia. *Global and Planetary Change*, 56:153–171.

Mejía-Navarro, M., E.E. Wohl, & S.D. Oaks. 1994. Geological hazards, vulnerability, and risk assessment using GIS: model for Glenwood Springs, Colorado. *Geomorphology*, 10: 331–354.

Mool, P.K, S.R. Bajracharya and S.P. Joshi, 2001. Inventory of glaciers, glacial lakes, and glacial lake outburst floods: Monitoring and early warning systems in the Hindu Kush-Himalayan regions. ICIMOD, Nepal.

Nagai, H. et al., 2016. Comparison of multiple glacier inventories with a new inventory derived from high-resolution ALOS imagery in the Bhutan Himalaya. *The Cryosphere,* 10.1: 65-85.

Nilsson, H. 2017. A dynamic and spatially distributed rainfall runoff model. MSc Thesis. Lund, Sweden: Lund University

O'Callaghan, J.F. & D.M. Mark. 1984. The extraction of drainage networks from digital elevation data. *Computer Vision, Graphics, and Image Processing*, 28: 323–344.

Osti, R., S. Egashira, & Y. Adikari. 2013. Prediction and assessment of multiple glacial lake outburst floods scenario in Pho Chu River basin, Bhutan. *Hydrological Processes*, 27: 262–274.

Papathoma-Köhle, M., M. Kappes, M. Keiler, and T. Glade. 2011. Physical vulnerability assessment for alpine hazards: state of the art and future needs. *Natural Hazards,* 58: 645-680.

Pilesjö, P. & A. Hasan. 2014. A Triangular Form-based Multiple Flow Algorithm to Estimate Overland Flow Distribution and Accumulation on a Digital Elevation Model. *Transactions in GIS*, 18:108–124.

Portocarrero, C., 2014. The Glacial Lake Handbook: Reducing Risk From Dangerous Glacial Lakes. The Mountain Institute and Engility Corporation, USAID Technical Report, Washington DC.

Post, A., and L.R. Mayo, 1971. Glacier dammed lakes and outburst floods in Alaska: U.S. Geological Survey Hydrologic Investigations Atlas.

Quincey, D.J. et al. 2007. Early recognition of glacial lake hazards in the Himalaya using remote sensing datasets. *Global and Planetary Change*, 56: 137–152.

Quinn, P. F., K. J. Beven, P. Chevallier, and O. Planchon. 1991. The prediction of hillslope paths for distributed hydrological modelling using digital terrain models. *Hydrological Processes*, 5: 59–79.

Ramsbottom D, Wade S, Bain V, Hassan M, Penning-Rowsell E, Wilson T, Fernandez A, House M, Floyd P., 2006. Flood risks to people: Phase 2. R&D Technical Report FD2321/IR2, *Department for the Environment, Food and Rural Affairs (DEFRA),* UK Environment Agency.

Richardson, S.D. & J.M. Reynolds. 2000. An overview of glacial hazards in the

Himalayas. *Quaternary International*, 65–66: 31–47.

Rivas, D.S. et al. 2015. Predicting outflow induced by moraine failure in glacial lakes: The Lake Palcacocha case from an uncertainty perspective. *Natural Hazards and Earth System Sciences*, 15: 1163–1179.

Rounce, D.R. et al., 2016. A new remote hazard and risk assessment framework for glacial lakes in the Nepal Himalaya. *Hydrology and Earth System Sciences*, 20: 3455–3475.

Rothacher D. and T. Watanbe, 1996. The 1994 Lugge Tsho Glacial Lake Outburst Flood, Bhutan Himalaya. *International Mountain Society*, 16: 77–81.

Schmidt J. et al. 2011. Quantitative multi-risk analysis for natural hazards: a framework for multi-risk modelling. *Natural Hazards*, 58: 1169–1192

Schomacker, A., 2011. Moraine. In *Encyclopedia of Snow, Ice and Glaciers, eds* V. P. Singh, P. Singh, & U. K. Haritashya, pp. 747–756. Dordrecht: Springer Netherlands.

Shrestha, A., 2005. Vulnerability assessment of weather disasters in Syangja district, Nepal : a case study in Putalibazaar Municipality, Department of Hydrology and Meteorology, Nepal.

Shrestha, A. B., M. Eriksson, P. Mool, P. Ghimire, B. Mishra, and N. R. Khanal. 2010. Glacial Lake Outburst Flood Risk Assessment of Sun Koshi Basin, Nepal. *Geomatics, Natural Hazards and Risk*, 1: 157–69.

Strategic Assessment Report, 2009. Bhutan National Environment Commission. https://www.internationalrivers.org/sites/default/files/attached-files/sia_punatsangchhu.pdf

Tadono, T. et al. 2012. Development and validation of new glacial lake inventory in the Bhutan Himalayas using ALOS 'DAICHI.'. *Global Environmental Research*, 16.1: 31-40.

Tweed, F. S. & J. L. Carrivick. 2015. Deglaciation and proglacial lakes. *Geology Today*, 31: 96-102.

Ukita, J., et al., 2011. Glacial lake inventory of Bhutan using ALOS data: methods and preliminary results. *Annals of Glaciology* 52.58: 65-71.

Veettil, B.K. et al. 2016. Glacier changes and related glacial lake expansion in the Bhutan Himalaya, 1990-2010. *Regional Environmental Change*, 16:1267–1278.

Vilímek, V. et al. 2014. Database of glacial lake outburst floods (GLOFs)-IPL project No. 179. *Landslides*, 11: 161–165.

Vilímek, V. et al. 2015. Geomorphologic impacts of the glacial lake outburst flood

from Lake No. 513 (Peru). *Environmental Earth Sciences,* 73: 5233–5244.

Vuichard, D. & M. Zimmerman. 1987. The 1985 catastrophic drainage of a moraine-dammed lake, Khumbu Himal, Nepal: cause and consequences. *Mountain Research and Development,* 7: 91–110.

Wang, S., D. Qin, & C. Xiao. 2015. Moraine-dammed lake distribution and outburst flood risk in the Chinese Himalaya. *Journal of Glaciology*, 61: 115–126.

Ward, A. D. & W. J. Elliot. 1995. *Environmental Hydrology.* CRC Press LLC.

Wang, W. et al. 2011. A first-order method to identify potentially dangerous glacial lakes in a region of the Southeastern Tibetan Plateau. *Mountain Research and Development*, 31: 122–130.

Wang, W., X. Yang, & T. Yao. 2012. Evaluation of ASTER GDEM and SRTM and their suitability in hydraulic modelling of a glacial lake outburst flood in southeast Tibet. *Hydrological Processes*, 26: 213–225.

Wang, X. et al. 2012. An approach for estimating the breach probabilities of moraine-dammed lakes in the Chinese Himalayas using remote-sensing data. *Natural Hazards and Earth System Science*, 12: 3109–3122.

Wang, W., Y. Gao, P. Iribarren Anacona, Y. Lei, Y. Xiang, G. Zhang, S. Li, and A. Lu. 2015. Integrated hazard assessment of Cirenmaco glacial lake in Zhangzangbo valley, Central Himalayas. *Geomorphology*. doi:10.1016/j.geomorph.2015.08.013.

Westoby, M.J. et al. 2014a. Modelling outburst floods from moraine-dammed glacial lakes. *Earth-Science Reviews*, 134: 137–159.

Westoby, M.J. et al., 2014b. Numerical modelling of Glacial Lake Outburst Floods using physically based dam-breach models. *Earth Surface Dynamics Discussions*, 2: 477–533.

Worni, R., C. Huggel, & M. Stoffel. 2013. Glacial lakes in the Indian Himalayas-from an area-wide glacial lake inventory to on-site and modeling based risk assessment of critical glacial lakes. *The Science of the total environment*, 468–469: S71-84.

Worni, R., C. Huggel, J. J. Clague, Y. Schaub, & M. Stoffel, 2014. Coupling glacial lake impact, dam breach, and flood processes: A modeling perspective. *Geomorphology*, 224: 161–176.

Yao, X. et al. 2012. Volume calculation and analysis of the changes in moraine-dammed lakes in the north Himalaya: A case study of Longbasaba

lake. *Journal of Glaciology*, 58: 753–760.

Zhang, G., T. Yao, H. Xie, W. Wang, and W. Yang. 2015. An inventory of glacial lakes in the Third Pole region and their changes in response to global warming. *Global and Planetary Change*, 131: 148–157. doi:10.1016/j.gloplacha.2015.05.013.

8 Appendices

8.1 Appendix A – Pho Chu lakes

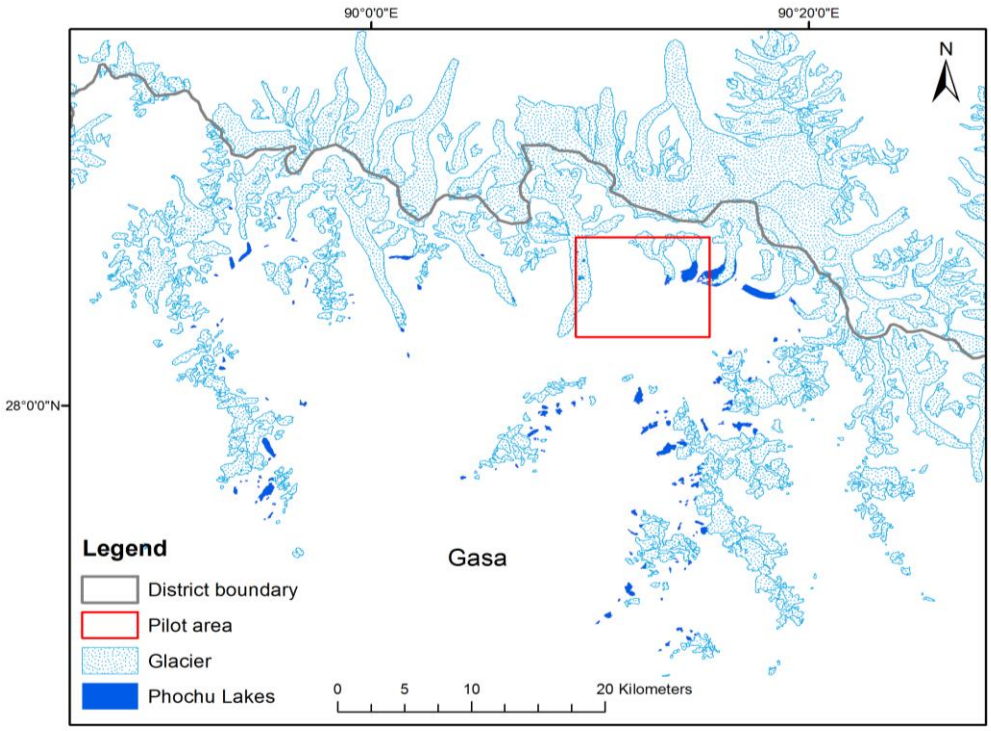

Figure A1. Glacial lakes in the Pho Chu sub-basin in the Himalayan region, Bhutan. Source: Glacier and Glacial Lake Inventory of Bhutan using ALOS Data (Version 16.11), JAXA.

8.2 Appendix B – Water depth snapshots

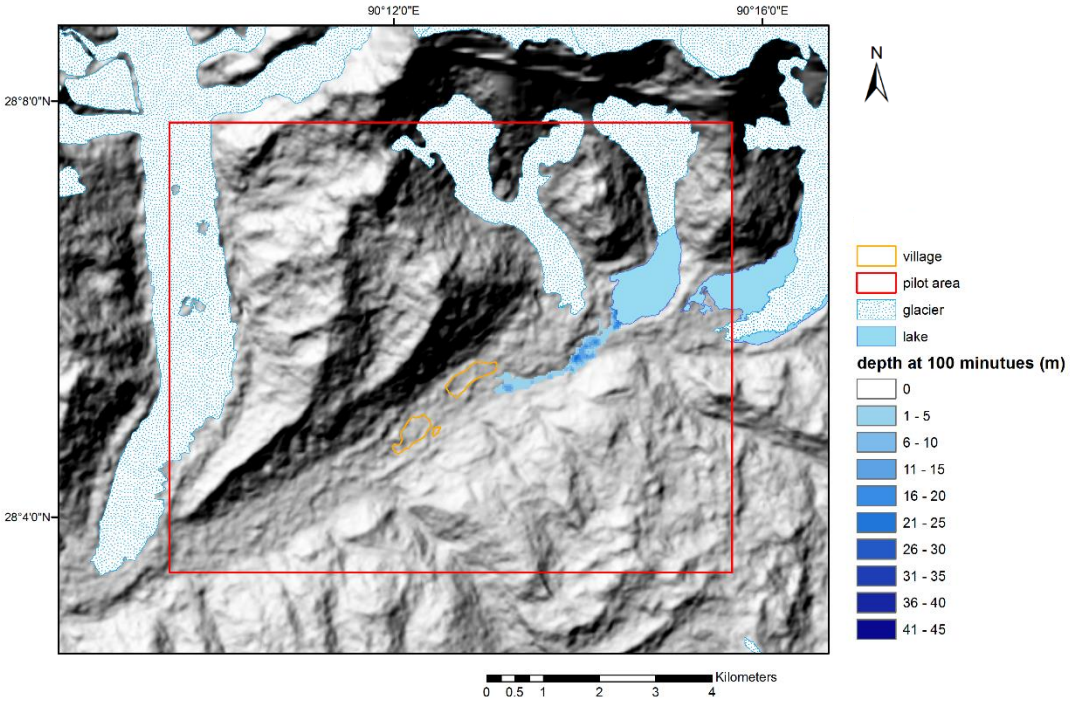

Figure B1. Water depth result at 100 minutes.

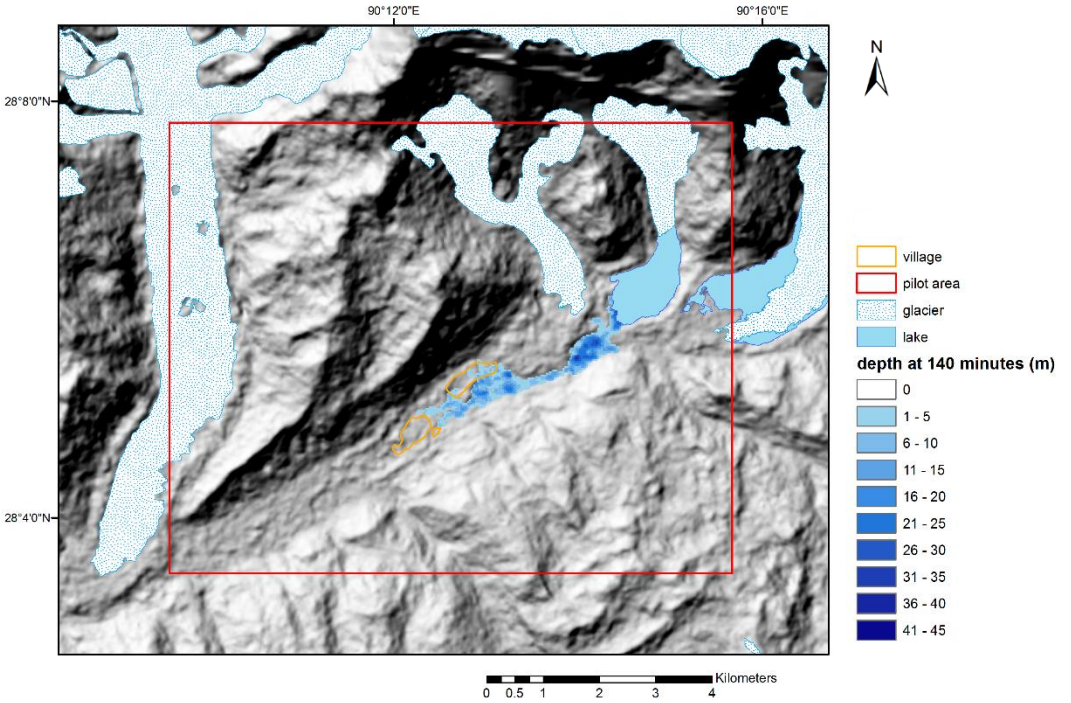

Figure B2. Water depth result at 140 minutes.

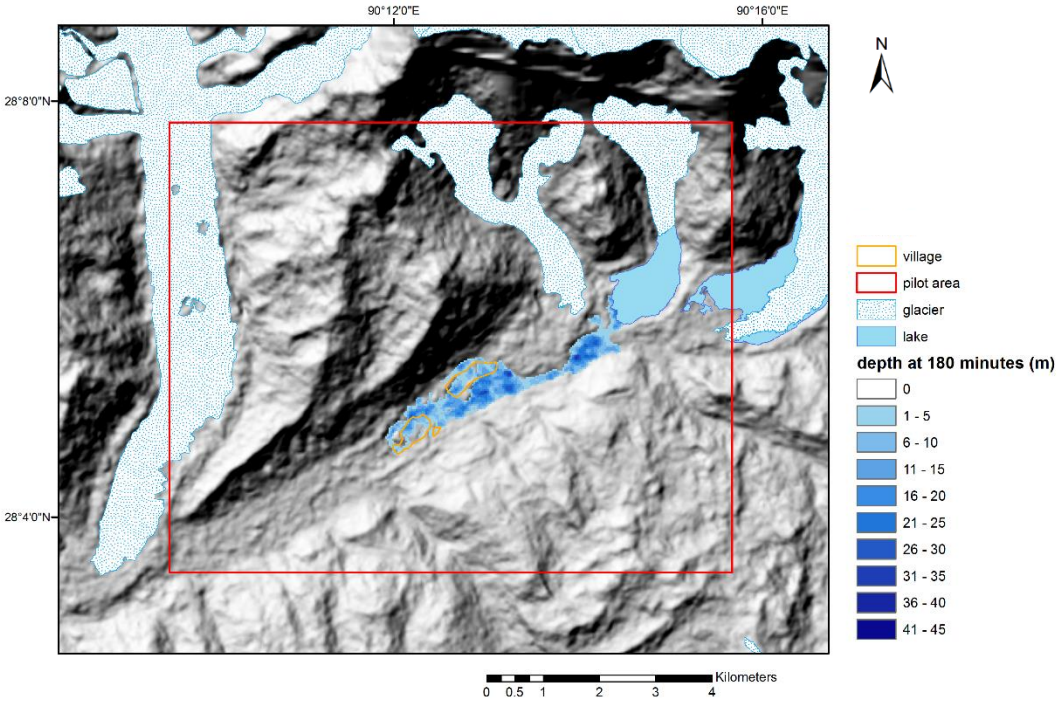

Figure B3. Water depth result at 180 minutes.

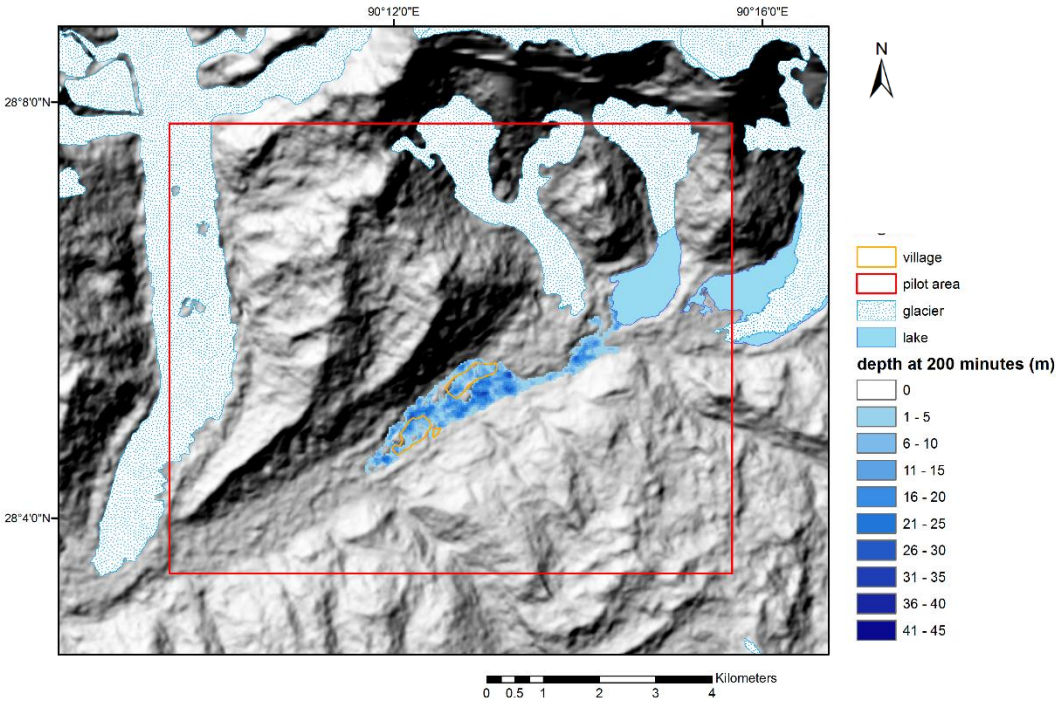

Figure B4. Water depth result at 200 minutes.

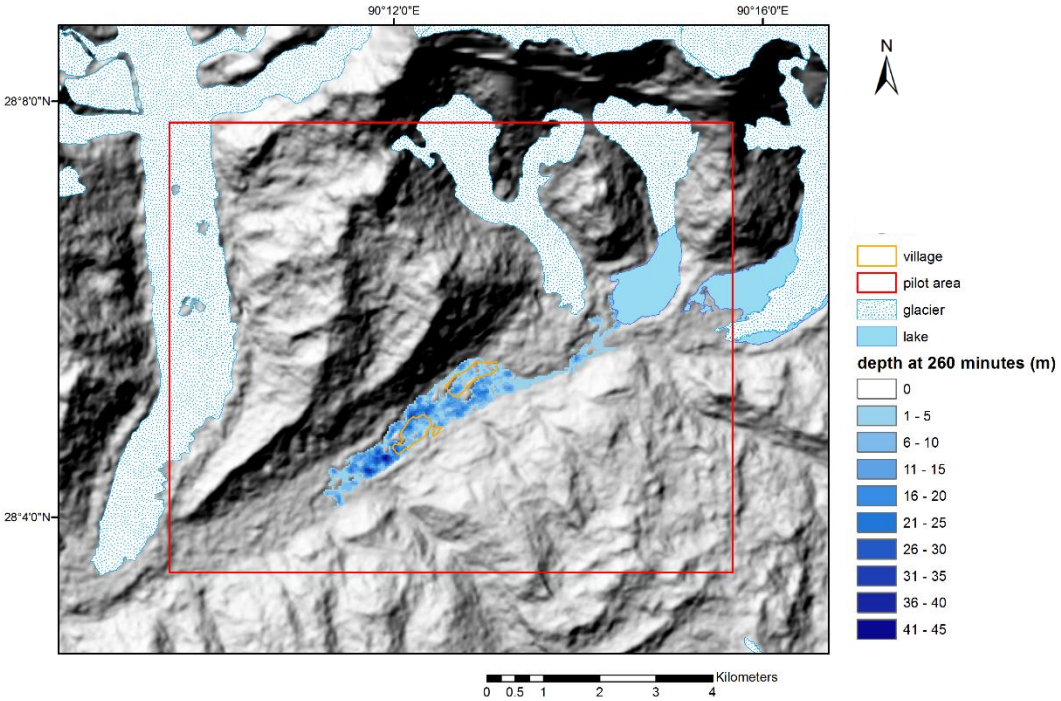

Figure B5. Water depth result at 260 minutes.

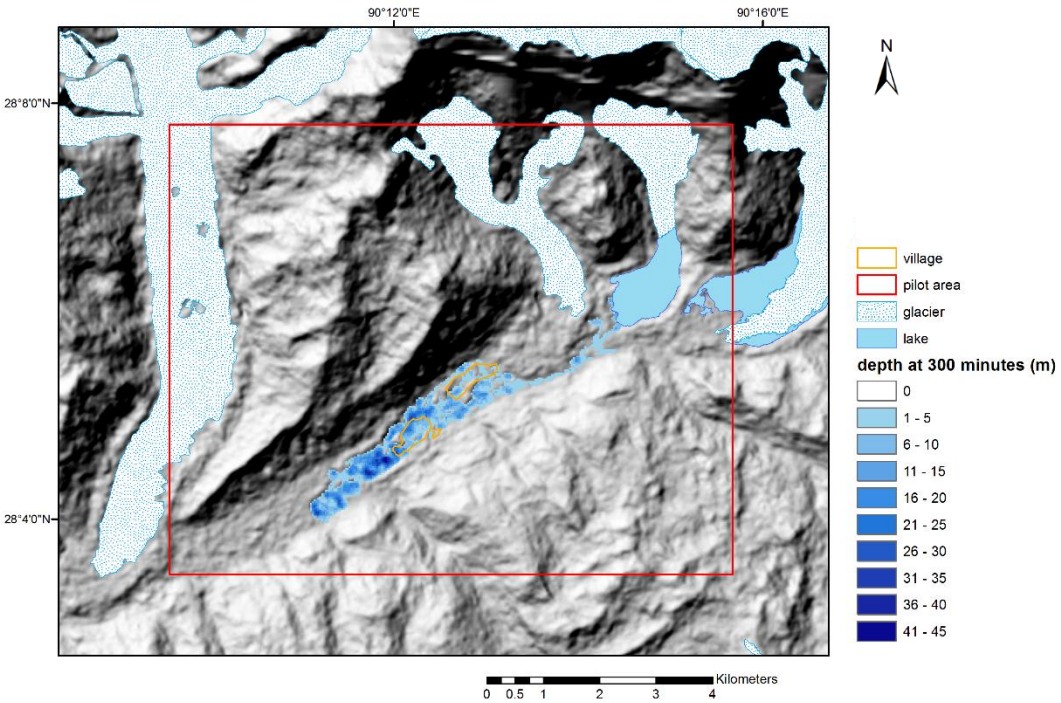

Figure B6. Water depth result at 300 minutes.

Department of Physical Geography and Ecosystem Science, Lund University

Lund University GEM thesis series are master theses written by students of the international master program on Geo-information Science and Earth Observation for Environmental Modelling and Management (GEM). The program is a cooperation of EU universities in Iceland, the Netherlands, Poland, Sweden and UK, as well a partner university in Australia. In this series only master thesis are included of students that performed their project at Lund University. Other theses of this program are available from the ITC, the Netherlands (www.gem-msc.org or www.itc.nl).

The student thesis reports are available at the Geo-Library, Department of Physical Geography and Ecosystem Science, University of Lund, Sölvegatan 12, S-223 62 Lund, Sweden. Report series started 2013. The complete list and electronic versions are also electronic available at the LUP student papers (https://lup.lub.lu.se/student-papers/search/) and through the Geo-library (www.geobib.lu.se).

1 Soheila Youneszadeh Jalili (2013) The effect of land use on land surface temperature in the Netherlands
2 Oskar Löfgren (2013) Using Worldview-2 satellite imagery to detect indicators of high species diversity in grasslands
3 Yang Zhou (2013) Inter-annual memory effects between Soil Moisture and NDVI in the Sahel
4 Efren Lopez Blanco (2014) Assessing the potential of embedding vegetation dynamics into a fire behaviour model: LPJ-GUESS-FARSITE
5 Anna Movsisyan (2014) Climate change impact on water and temperature conditions of forest soils: A case study related to the Swedish forestry sector
6 Liliana Carolina Castillo Villamor (2015) Technical assessment of GeoSUR and comparison with INSPIRE experience in the context of an environmental vulnerability analysis using GeoSUR data
7 Hossein Maazallahi (2015) Switching to the “Golden Age of Natural Gas” with a Focus on Shale Gas Exploitation: A Possible Bridge to Mitigate Climate Change?
8 Mohan Dev Joshi (2015) Impacts of Climate Change on *Abies spectabilis*: An approach integrating Maxent Model (MAXent) and Dynamic Vegetation Model (LPJ-GUESS)
9 Altaaf Mechiche-Alami (2015) Modelling future wheat yields in Spain with LPJ-GUESS and assessing the impacts of earlier planting dates
10 Koffi Unwana Saturday (2015) Petroleum activities, wetland utilization and livelihood changes in Southern Akwa Ibom State, Nigeria: 2003-2015
11 José Ignacio Díaz González (2016) Multi-objective optimisation algorithms for GIS-based multi-criteria decision analysis: an application for evacuation planning

12 Gunjan Sharma (2016) Land surface phenology as an indicator of performance of conservation policies like Natura2000
13 Chao Yang (2016) A Comparison of Four Methods of Diseases Mapping
14 Xinyi Dai (2016) Dam site selection using an integrated method of AHP and GIS for decision making support in Bortala, Northwest China
15 Jialong Duanmu (2016) A multi-scale based method for estimating coniferous forest aboveground biomass using low density airborne LiDAR data
16 Tanyaradzwa J. N. Muswera (2016) Modelling maize (Zea Mays L.) phenology using seasonal climate forecasts
17 Maria Angela Dissegna (2016) Improvement of the GPP estimations for Sudan using the evaporative fraction as water stress factor
18 Miguel G. Castro Gómez (2017) Joint use of Sentinel-1 and Sentinel-2 for land cover classification: A machine learning approach
19 Krishna Lamsal (2017) Identifying potential critical transitions in a forest ecosystem using satellite data
20 Maimoona Zehra Jawaid (2017) Glacial lake flood hazard assessment and modelling: a GIS perspective